Contract Report CERC-96-1
September 1996

US Army Corps of Engineers
Waterways Experiment Station

Coherent Acoustic Sediment Flux Probe

by T. P. Stanton
Naval Postgraduate School

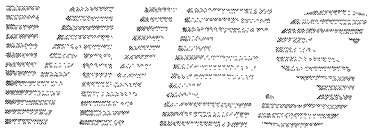

Prepared for Headquarters, U.S. Army Corps of Engineers

Contract Report CERC-96-1
September 1996

Coherent Acoustic Sediment Flux Probe

by T. P. Stanton

Naval Postgraduate School
Monterey, CA 93943

Final report

Approved for public release; distribution is unlimited

Prepared for U.S. Army Corps of Engineers
Washington, DC 20314-1000

Monitored by U.S. Army Engineer Waterways Experiment Station
3909 Halls Ferry Road
Vicksburg, MS 39180-6199

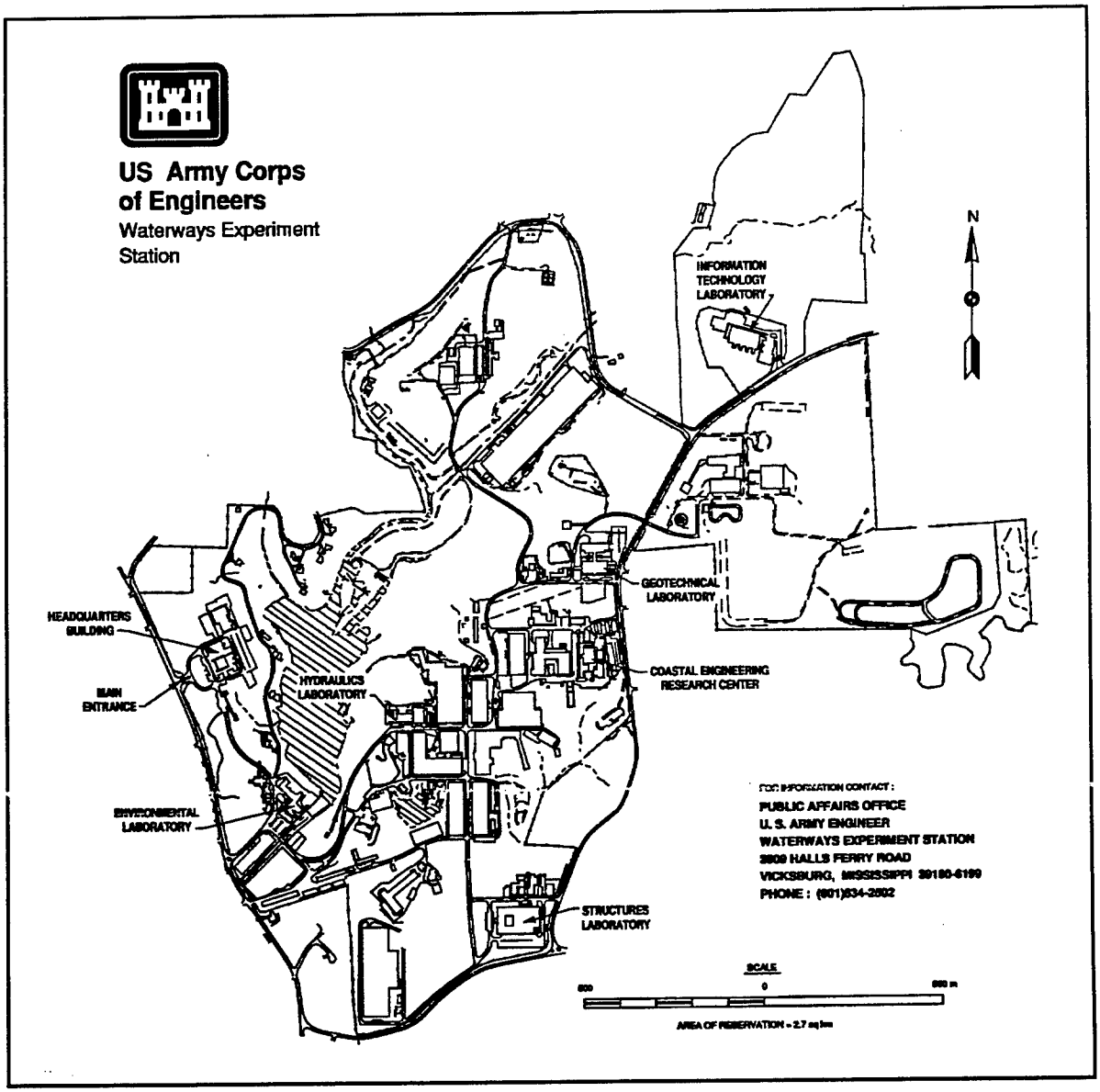

Waterways Experiment Station Cataloging-in-Publication Data

Stanton, T. P.

Coherent acoustic sediment flux probe / by T. P. Stanton ; prepared for U.S. Army Corps of Engineers ; monitored by U.S. Army Engineer Waterways Experiment Station.

74 p. : ill. ; 28 cm. — (Contract report ; CERC-96-1)

Includes bibliographical references.

1. Probes (Electronic instruments) 2. Doppler effect. 3. Acoustic imaging. 4. Suspended sediments — Measurement. I. United States. Army. Corps of Engineers. II. U.S. Army Engineer Waterways Experiment Station. III. Coastal Engineering Research Center (U.S. Army Engineer Waterways Experiment Station) IV. Title. V. Series: Contract report (U.S. Army Engineer Waterways Experiment Station) ; CERC-96-1.

TA7 W34c no.CERC-96-1

Contents

Preface

This is a contract final report on the development of a new sediment-flux sensor, the coherent acoustic sediment-flux probe (CASP). The sediment flux instrumentation described in this report was funded under contract No. MIPR W81EWF-3-CO30 and W81EWF-2-C116 with the U.S. Army Engineer Waterways Experiment Station's (WES) Coastal Engineering Research Center (CERC) as part of work unit 32532, "Sediment Transport Instrumentation for the Littoral Environ-ment," in the Coastal Engineering Research Program.

The rapid development of the CASP has been possible due to prior scientific and engineering work supported by the Office of Naval Research small-scale physical oceanography division. This development and its extension into the CASP sediment flux probe has been a group effort. Acknowledgement is due to Mr. Rob Wyland for the mechanical design and implementation of the package and calibration tank, Mr. Jim Stockel for the DSP code development and postprocessing software, Messrs. Larry Blalock and Jeff Helmes for assembling the electronic boards and cabling, and Mr. Jim Lambert for machining the test facility components. Different elements of the CASP development were the subject of four Naval Postgraduate School Masters theses. LT E. Coehlo, LT W. Anderson, LT K. Kahanowich, and LT T. McIntyre have all made significant contributions to the acoustic calibration of the CASP system.

This report was written by Mr. T. P. Stanton, Naval Postgraduate School. Technical oversight and cooperation were performed by Professor Edward Thornton of the Naval Postgraduate School and the project Principal Investigator, Dr. Thomas E. White, at CERC. The CERC technical review committee providing technical guidance consisted of Drs. White and Todd Walton, and Mr. Gary Howell.

WES supervisors during this report's preparation were Branch Chief, William L. Preslan; Division Chief, Thomas W. Richardson; Program Manager, Carolyn M. Holmes; Assistant Director, CERC, Charles C. Calhoun, Jr.; Director, CERC, Dr. James R. Houston; Director of WES, Dr. Robert W. Whalin, and Commander of WES, COL Bruce K. Howard, EN.

1 Introduction

A high resolution, 3 component sediment flux probe has been developed to meet the objectives outlined by the National Academy of Science Panel on Coastal Engineering Measurements (White letter, 26 Sep 1991), using very high frequency coherent acoustic doppler techniques. The Coherent Acoustic Sediment Flux Probe (CASP) has been designed to meet the following considerations defined by the panel:

° nonintrusive sensor: remotely measures velocity and sediment concentration

° measure sediment mass-flux: measures all three velocity components and infers sediment concentration from backscatter strength from the same sample volume

° measure sediment size: infers size using two backscattered acoustic frequencies

° field ready instrument: instrument has already been field tested

° compatible with SAUSDAS: three velocity components and mass concentration at a primary sample volume are output in a format compatible with the SAUSDAS

° The instrument will be operational, calibrated and field tested prior to August 1994 in time for implementation in the DUCK 94 experiment.

As the CASP measures the full velocity vector at the 0.6 cm^3 scale primary sample volume, dynamically important turbulent parameters such as the Reynolds stress timeseries can also be determined at the measurement site. In a wave driven environment, the importance of a full three component velocity measurement at the same point that sediment mass estimates are made can be seen in the following conceptual framework for suspended sediment flux. Velocities and sediment concentration are partitioned into mean and perturbed parts, where the perturbed part in this case is composed of both wave and turbulent contributions, and will have non-zero covariances. The conservation of sediments, M, is given by (see for example Bedford et al, 1987)

$$\frac{\partial \overline{M}}{\partial t}+\frac{\partial \overline{U_j M}}{\partial x_j}-W_s\frac{\partial \overline{M}}{\partial z}=K\frac{\partial^2 \overline{M}}{\partial x_j^2}-\frac{\partial}{\partial x_j}\overline{(u'_j M')} \qquad j=1,2,3 \qquad (1)$$

where the three velocity components are described by $u_j=U_j+u'_j$, W_s is the vertical velocity of the sediments, K is the molecular diffusivity coefficient, and the overbars indicate time averaging. The equation states the storage and advection of sediments must be balanced by the molecular diffusivity and the divergences of turbulent sediment fluxes. Due to the large

Reynolds number encountered in the surf zone, the viscous terms may be generally ignored. In an environment where both strong turbulent stresses and irrotational flow associated with wave orbital motion may be present, it is important to fully resolve the three component velocity and flux vector so that the full covariance vector $\langle u'_j c' \rangle$ is estimated. The CASP has been designed to estimate velocity and concentration down to cm scales with sufficient temporal resolution to capture transient turbulent events associated with wave processes.

In this report, the acoustic, electronic, mechanical and signal processing implementations of the CASP are described, followed by an explanation of the doppler velocity and sediment concentration estimation techniques. Finally, examples of velocity, mass concentration and sediment fluxes from the DUCK94 experiment are shown.

2 Coherent Acoustic Sediment-flux Probe (CASP)

The CASP system consists of an underwater housing equipped with three 5.2 MHz acoustic transceivers, a single 1.4 MHz transceiver, a pair of precision tilt sensors to correct package orientation tilts, and electronic processing and control modules which output a high speed digital data stream to a shore based processing computer. The instrument package is typically positioned looking downward at the bottom boundary layer to sample the velocity vector and sediment flux vector at a primary measurement volume 25 cm in front of the instrument head. In addition, profiles of sediment concentration are estimated every 1.68 cm along each of the four narrow acoustic beams. During the deployment in Duck 94, the CASP was raised and lowered using a remotely controlled hydraulic arm which varied the height of the primary sample volume above the sediment bed (see Figure 1). This allowed vertical profiles of sediment fluxes to be estimated, and the local morphology to be determined from the along-beam bottom backscatter profiles over a 0.5 m^2 area.

Principals of operation and descriptions of the system components follow.

Acoustics

A combination of high resolution coherent doppler processing and both monostatic and bistatic acoustic sampling techniques are used in the CASP to estimate the three component velocity vector and sediment concentration at a single sample volume in front of the acoustic transducers. Three 5.2MHz transducers are embedded in the ends of 10 cm long arms mounted radially out from the instrument head (see the schematics in Figures 1 and 2), such that the narrow, 2.5° width beams intersect at a point 25 cm in front of the head. In the bistatic mode, one of the three 5.2 MHz transducers emits a series of 32 short (0.5 cm length bins in water), acoustic pulses into the water column, while the other two transducers "listen" to acoustic energy backscattered from particulates at the beam intersection volume. The schematic in Figure 2 illustrates this bistatic mode of operation. The received backscattered signals are amplified and downshifted by a homodyning, complex output mixer, then sampled coherently only at the primary sample volume by using a precise delay timed from the start of the transmitted acoustic pulse. After 32 complex amplitude samples have been coherently sampled from both receiving transducers, the transducers are electronically switched such that another transducer is transmitting while the remaining two transducers receive. This round-robin sequence is rapidly repeated such that each of the three transducers has been a transmitter, giving six sets of complex amplitude estimates from which the velocity components can be estimated (see section 3).

A monostatic sampling mode is interleaved into this sequence to estimate the along-

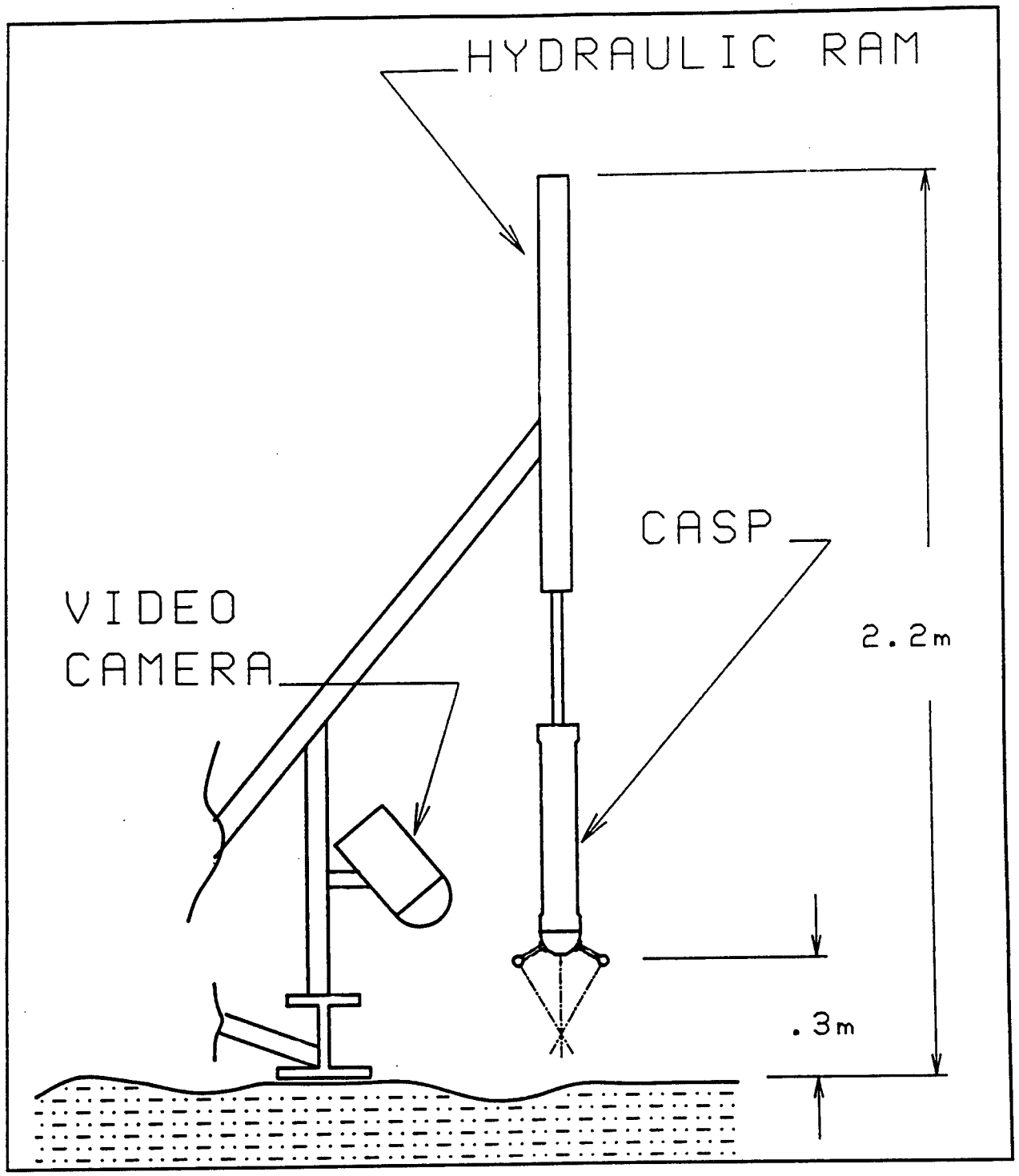

Figure 1. Typical deployment configuration for the CASP probe looking at a nearshore sediment bed. The probe is lowered and raised mechanically to profile velocity and sediment fluxes through the water column.

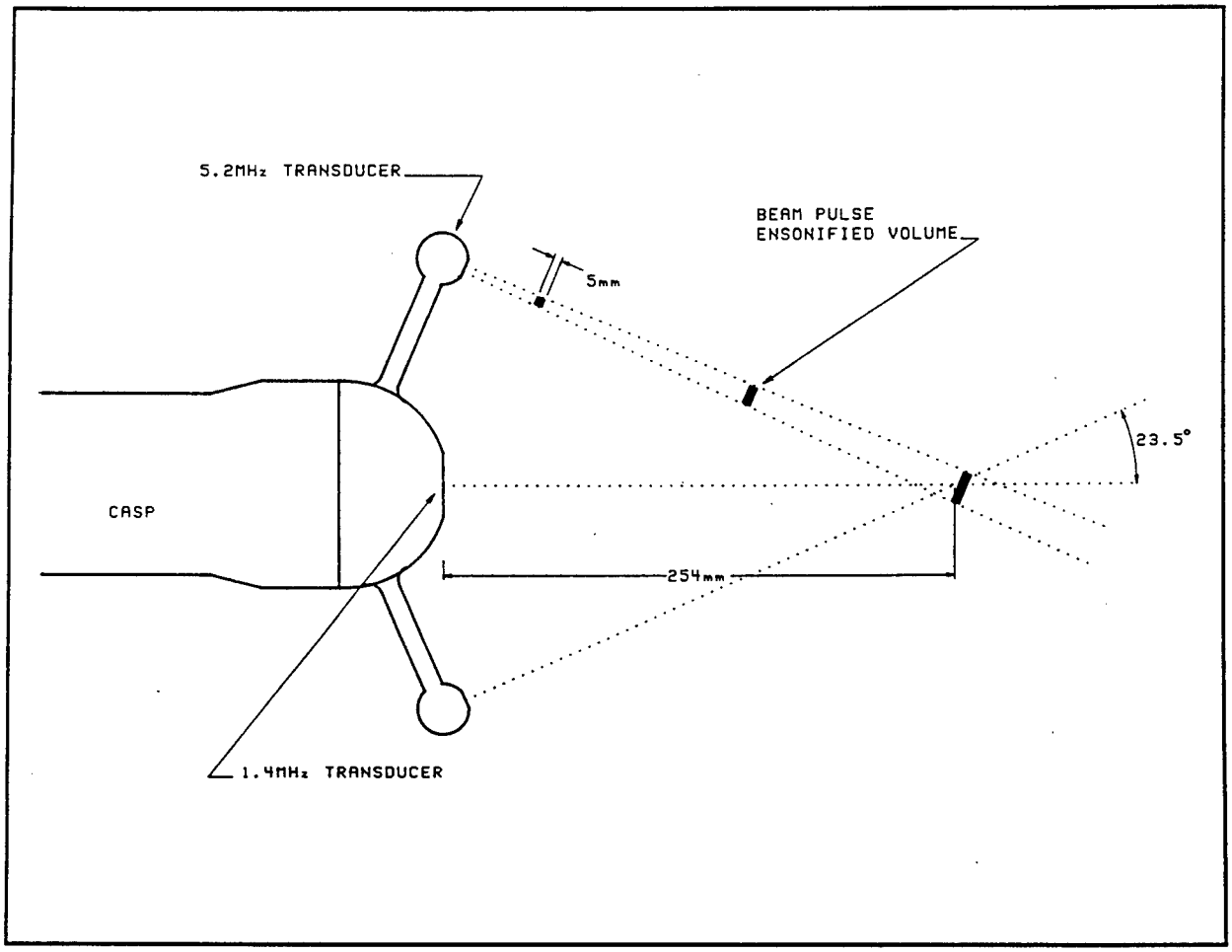

Figure 2. Schematic of the bistatic mode of the acoustic transducers on the CASP. One of the three transducers transmits a series of short acoustic pulses while the other two receive signals backscattered from the intersection volume of the 3 narrow beams.

beam backscatter intensity for the three 5.2 MHz transducers and single 1.4 MHz unit. In this mode, a triplet of longer (1.6 cm range bin) duration pulses are transmitted from each transducer in sequence. As soon as each transmitted pulse is completed, the transducer is immediately switched to the receive mode, and the complex backscatter amplitudes sampled every 1.7 cm out to a range of 1.2 m. This full sequence of three bistatic and three monostatic transmit modes is continuously repeated at a 36 Hz rate.

In summary, the hybrid acoustic sampling system provides the following data:

- 3 transducer, 5.2 MHz backscatter bistatic mode acoustic doppler system:
  - (u,v,w) and backscatter intensity at 36 Hz within a 0.6 cm^3 sampling volume, 25 cm in front of the probe.
  - along-beam backscatter intensity every 1.7 cm out to 1.2 m at 4 Hz (all 3 beams).

- Single downward looking 1.4 MHz backscatter acoustic system:
  - along-beam velocity and backscatter intensity every 1.7 cm from a O(1 cm^3) sample volume bin at 4 Hz.
  - range to the sediment bed to 1.6cm resolution.

Electronics processing

A block diagram of the electronic processing components in the CASP system is shown Figure 3. A summary of the major subsystems in this schematic, working from left to right, follows.

Each of the four acoustic transducers is connected to a transceiver module which contains a high power pulsed transmitter, electronic transceive switching, and a bandpassed gain stage. Packets of sinusoidal acoustic waves are generated by the transmitter circuits using control signals and clock frequencies generated by the acoustics sequencer/controller board. Backscattered acoustic signals received by each transducer pass through a high gain, wide dynamic range amplifier which drives in-phase and quadrature mixers. These mixers shift the received ultrasonic signals to base-band frequencies which represent doppler shifts of the transmitted frequency due to the movement of the acoustic scatterers. The complex amplitude signals from each transducer are then sampled by fast sample and hold circuits at pre-programmed delays timed from the transmit pulse. This raw, coherently sampled acoustic data stream is subsequently used to estimate the doppler velocity shifts and backscatter amplitudes. All four transceivers and the sequencer/controller/clock generator are interconnected by a 26-line bus carrying powersupplies, sampled signals, clocks and control lines.

All timing and clock signals for the system are generated synchronously on the sequencer/controller/clock generation board, which interconnects the acoustic front end and

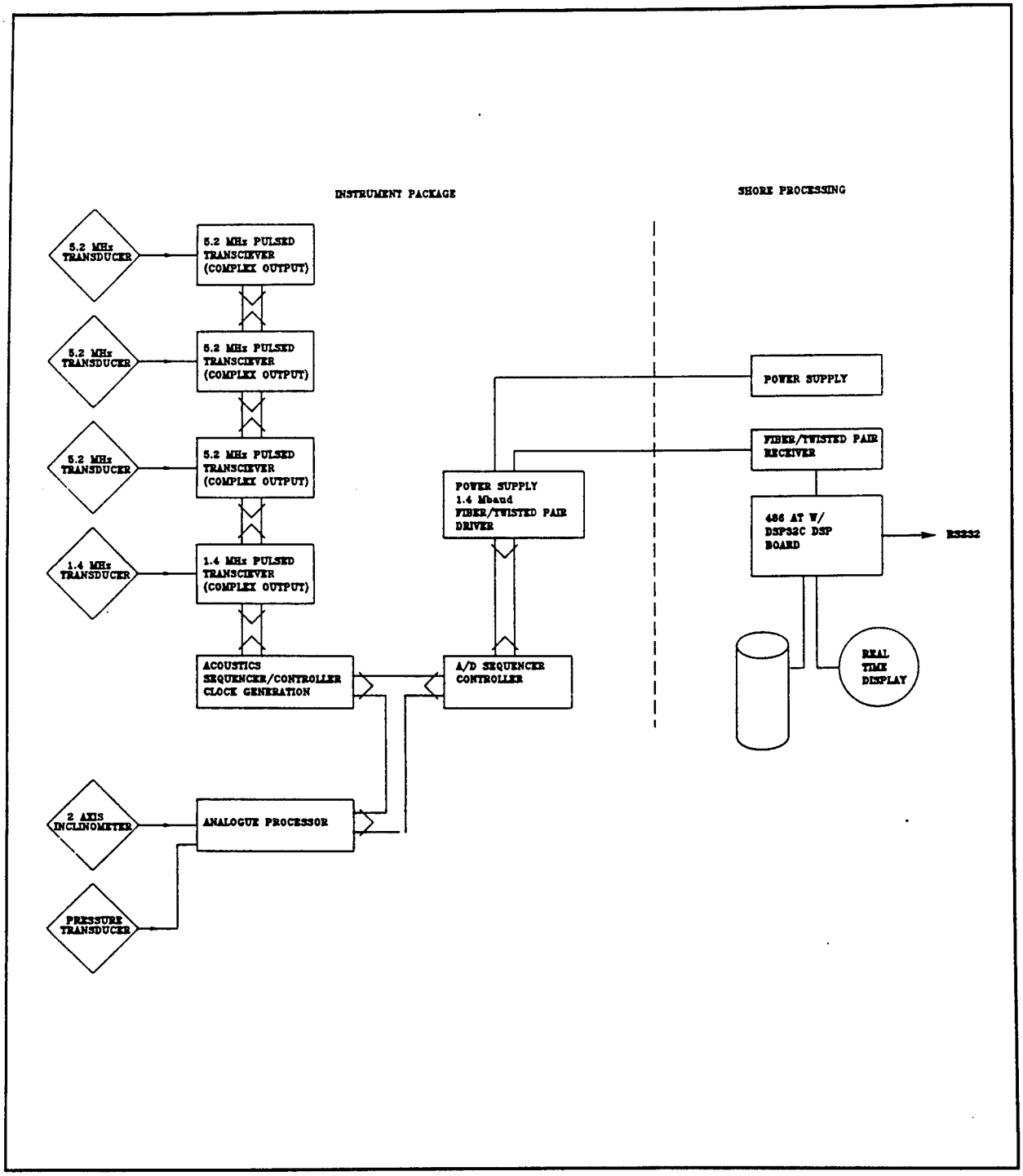

Figure 3. Schematic of the electronic processing sub-systems in the CASP. Transducers are shown on the left side and shore processing on the right side.

main A/D buses. This common clock design ensures that all the transmit frequencies, transmit control and sampling pulses are phase synchronous to meet the stringent phase coherent sampling requirements and to minimize asynchronous digital noise sources interfering with the very sensitive acoustic front end amplifiers. An erasable programmable read only memory (EPROM) is used to store the complicated transmit and sample patterns for the transceiver modules required to achieve the hybrid monostatic and bistatic sampling sequence described in section 2.1. This transmit control and sampling sequence is also synchronized with the programmable analogue multiplexer on the A/D sequencer board. A programming environment has been written on an HP workstation to flexibly generate the control sequences based on specified sampling strategies. The output code can be ported to an EPROM programmer, and the software also generates control files used by the analysis software to interpret the CASP data stream.

Several environmental variables are measured within the CASP and digitized into the outbound data stream to help interpret the doppler velocity data. As the orientation of the sediment flux probe must be known to transform the measured three component vector quantities into an earth-referenced coordinate system, a 0.1° accuracy, two axis tilt sensor is mounted within the acoustic transducer head. A high resolution pressure transducer is mounted in the instrument head to provide instrument depth and an estimate first order wave height. These sensors are preconditioned, low-pass filtered then fed to the main data acquisition board.

Analogue signals from the acoustic transceivers and ancillary sensors are passed across the analogue bus along with power supply lines and control signals to the A/D sequencer/controller. Here, a second EPROM controls a 16 channel multiplexer, the acoustic front end sequencer cycling and the main digitized frame sequence. The multiplexed data are continuously digitized at an 88 KHz rate with 14 bit precision, and the digital data transferred to a high speed manchester encoder to provide self-clocking, synchronous, data transmission to the shore. This 1.4 Mbaud data stream can either be transmitted over a twisted wire pair for distances up to 100 m, or over a fiberoptic line up to 2 km.

The shore processing electronics consists of a power supply for the CASP instrument, a data receiver, and a 486 AT with a AT&T DSP32C digital signal processor (DSP). The DSP provides a 12 - 25 MFlop, floating point processing capability to receive, demultiplex and doppler process the fast inbound data stream in real time using code written largely in C. Manchester encoded digital data from the CASP is converted to a bit-serial format by the fiber/twisted pair receiver directly feeding an inbound Direct Memory Access (DMA) synchronous data port on the DSP chip. Under software control, data frames are synchronized and put into a rotary input buffer which the main DSP software can access. The data processing algorithms will be described in more detail in section 3 and 4. Frames of processed data are passed once every second to the "fore-ground" program running on the 486 DOS computer, where selected data can be plotted in real time and optionally stored to disk. The primary output data backscatter profiles (at up to 4 Hz) and raw doppler frequency estimates at 36 Hz. A postprocessing program (PostCASP) interprets these preprocessed and

stored timeseries and calculates sediment mass profiles and (u,v,w) velocity component timeseries in either a binary or ASCII format files. The configuration and operation of the software and interactive graphical interface are shown in a users guide in Appendix B, the data storage formats for DSP processed data are described in Appendix C, and the postprocessing program is documented in Appendix D .

Mechanical Design

To minimize flow disturbance and mechanical drag, the CASP has been designed to fit into the smallest package which could accommodate the transducers and processing electronics. The major mechanical components of the CASP are the transducer head, a light-weight internal chassis which supports the electronic sub-systems, a delryn (plastic) endcap with an underwater connector, and a machined, necked PVC plastic housing.

End and side-view schematics of the machined 316 stainless steel transducer head are shown in Figures 4 and 5 respectively. The 1.4 MHz transducer is mounted flush in the center of the head, while the three 5.2 MHz transducers, set in machined 316 stainless steel arms, mount radially out from the head such that their beam axes intersect 25 cm in front of the 1.4 MHz transducer. The pressure transducer and oil-filled diaphragm assembly are shown below the 1.4 MHz transducer in figure 4. The dual axis tilt sensor is mounted in the larger cavity at the base of the head (see figure 6). All the external transducer components have face O-ring seals, and the complete head assembly mates with the PVC housing with dual radial seals.

The internal mechanical layout of the CASP is shown in Figure 6. The complete package is approximately 70 cm long, and accommodates the four acoustic transceiver modules, the acoustic sequencer/controller, analogue processing board, and A/D board described in section 2.2. The ribbon cable buses interconnecting these processing systems allow relatively easy access to the components, despite the very compact construction. All the printed circuit boards (developed in-house under other programs) are double-sided, fiberglass boards with plated-through holes and solder masks, and use high quality, gold-plated connectors throughout.

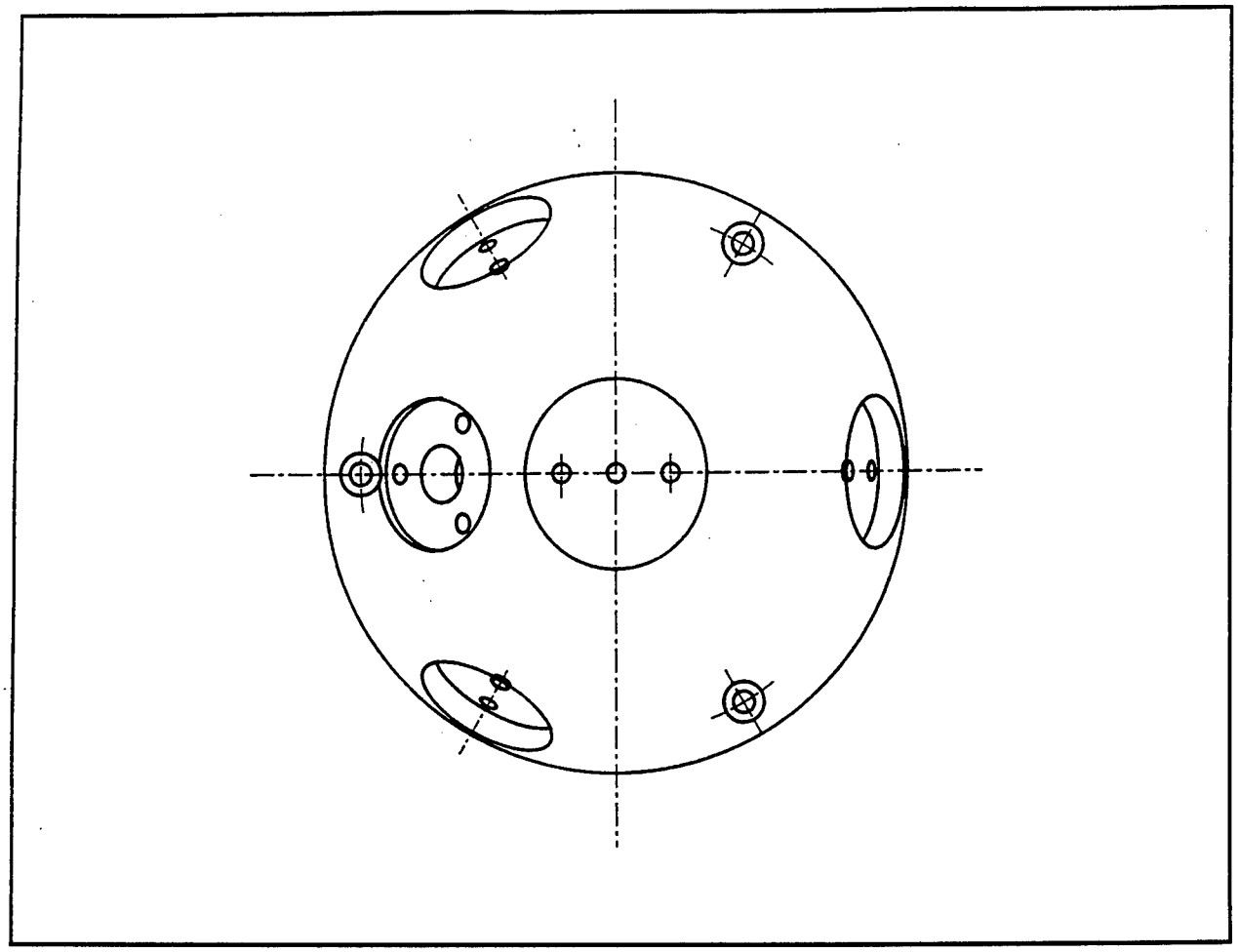

Figure 4. End view drawing of the CASP transducer head showing the central 1.4 MHz transducer well, three radially directed 5.2MHz arm transducer mount surfaces, and the pressure transducer diaphragm below the 1.4 MHz transducer.

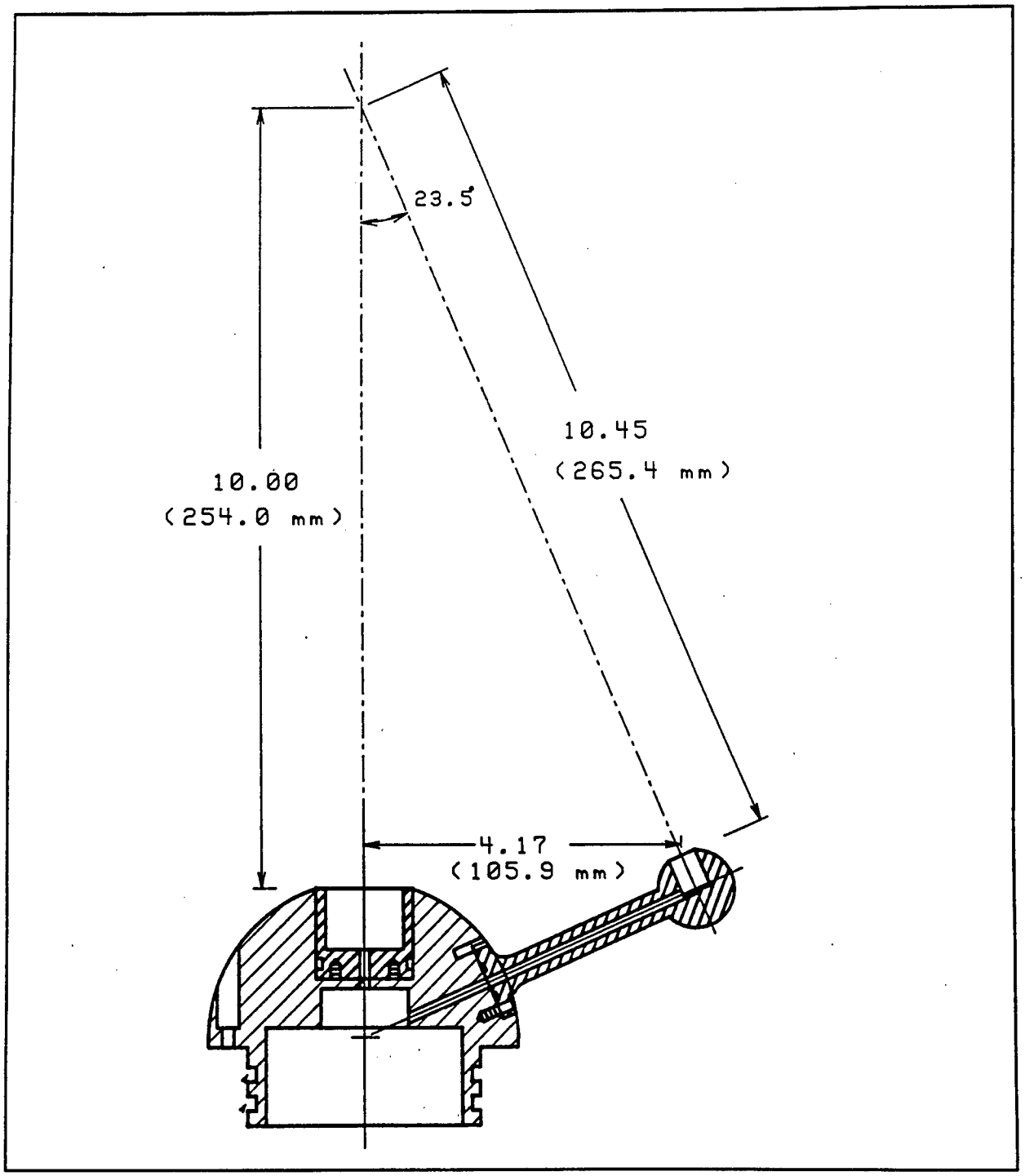

Figure 5. Side view drawing of the CASP transducer head. The 1.4 MHz transducer well is in the upper center of the head, and one of the three arm transducers is shown.

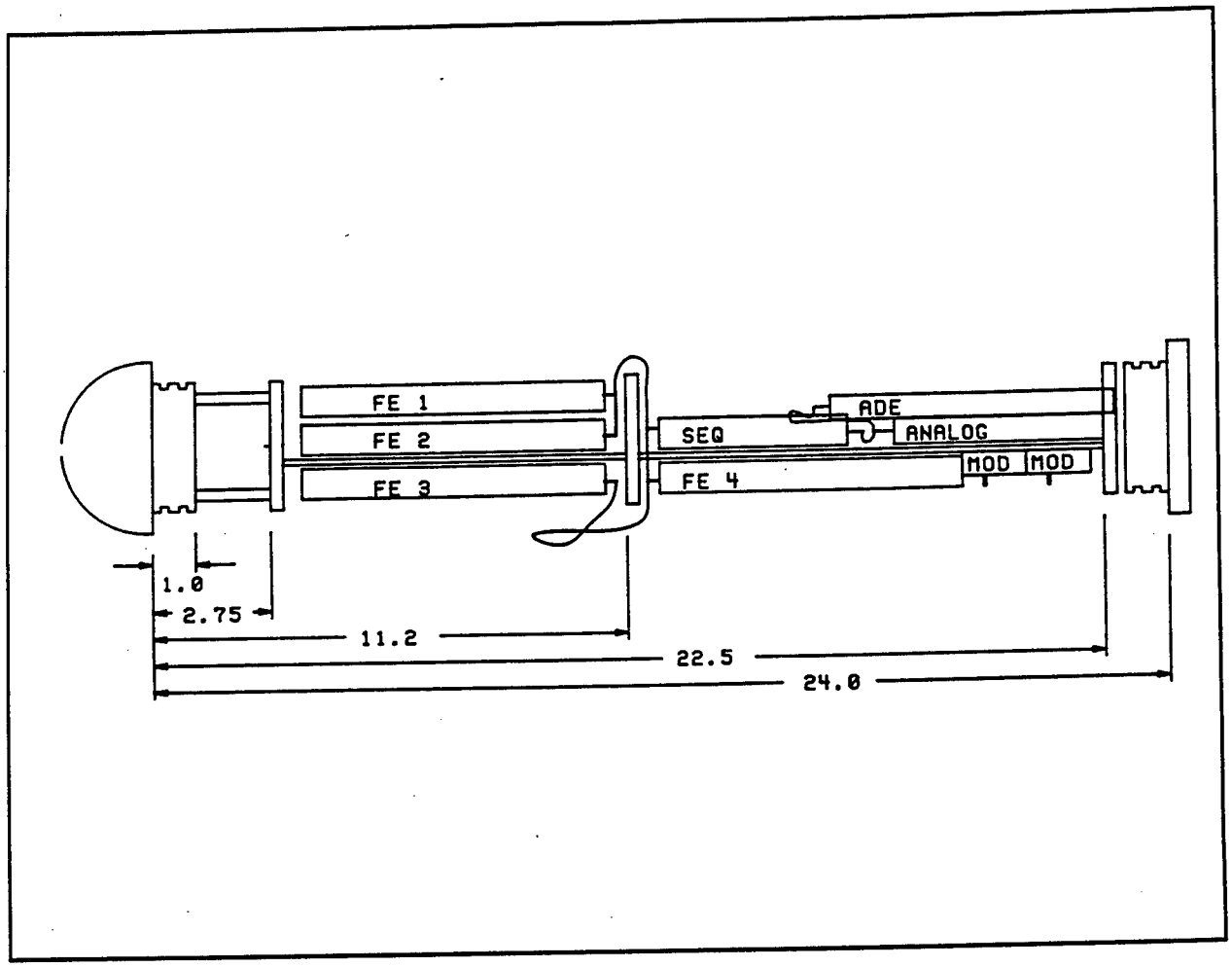

Figure 6. Drawing of the internal components of the CASP. Four Front End (FE) modules pre-process the acoustic data, the sequencer board (seq) controls the acoustic transmissions and sampling, the analog board preconditions ancillary transducers, and the ADE board digitizes the multiplexed data stream.

3 Doppler Velocity Measurements

The velocity component estimation in the acoustic bistatic mode is based on estimation of the mean doppler shift of the backscattered acoustic energy resulting from the relative velocity of scatterers present in the intersection volume. To obtain the velocity components from the received complex amplitude timeseries, the following steps are performed by the DSP, foreground program, and postprocessing programs:

1 - Demultiplex the blocks of complex acoustic data from the data stream.

2 - Apply doppler frequency estimators to the acoustic data blocks.

3 - Clear data of spikes using reciprocal channel comparison, received signal amplitude, and the estimated doppler bandwidths.

4 - Compute velocities from the doppler frequencies.

5 - Transform velocity estimates to an orthogonal frame of reference fixed to the instrument.

6 - Rotate velocity vectors to an absolute vertical reference frame.

The unique combined monostatic and bistatic measurement techniques used in the CASP required investigation of several doppler frequency estimation methods. The estimation of three component velocity vectors required a doppler frequency spectral estimator, working in real-time, which could use a small number of coherently sampled data points. In order to choose the most suitable algorithm, and to assess its performance, Monte-Carlo simulations were performed using several possible spectral estimators (Coelho, 1991). From the simulations described in more detail in Appendix E, the Pulse Pair algorithm, or equivalently the MUSIC order 2 algorithm, showed the best performance, followed by the Peak FFT algorithm. The FFT estimator is equivalent to a maximum likelihood estimator, but it's resolution is seriously degraded when there are a small number of input sample points. Using these results, the Pulse Pair estimator was implemented, together with the pre-processing of the other measured quantities, on the front-end Digital Signal Processor to provide real-time pre-processing and review of the raw doppler data.

The doppler velocity estimation can be considered for any two of the three transducers, where transducer 1 is transmitting and transducer 2 is receiving. Figure 7 shows the geometry for transducers T1 and T2, tilted in the plane formed by the transmitted acoustic beams. The very narrow (3° double-sided half power beam width) acoustic beams intersect at the primary scattering volume, labeled BS. An arbitrary velocity vector is shown as "True Velocity", with components v_{BS}^{T1} directed along the T1 acoustic beam axis and v_{BS}^{T2} long the T1 beam. Assuming that the equipment is in a fixed frame, the following doppler

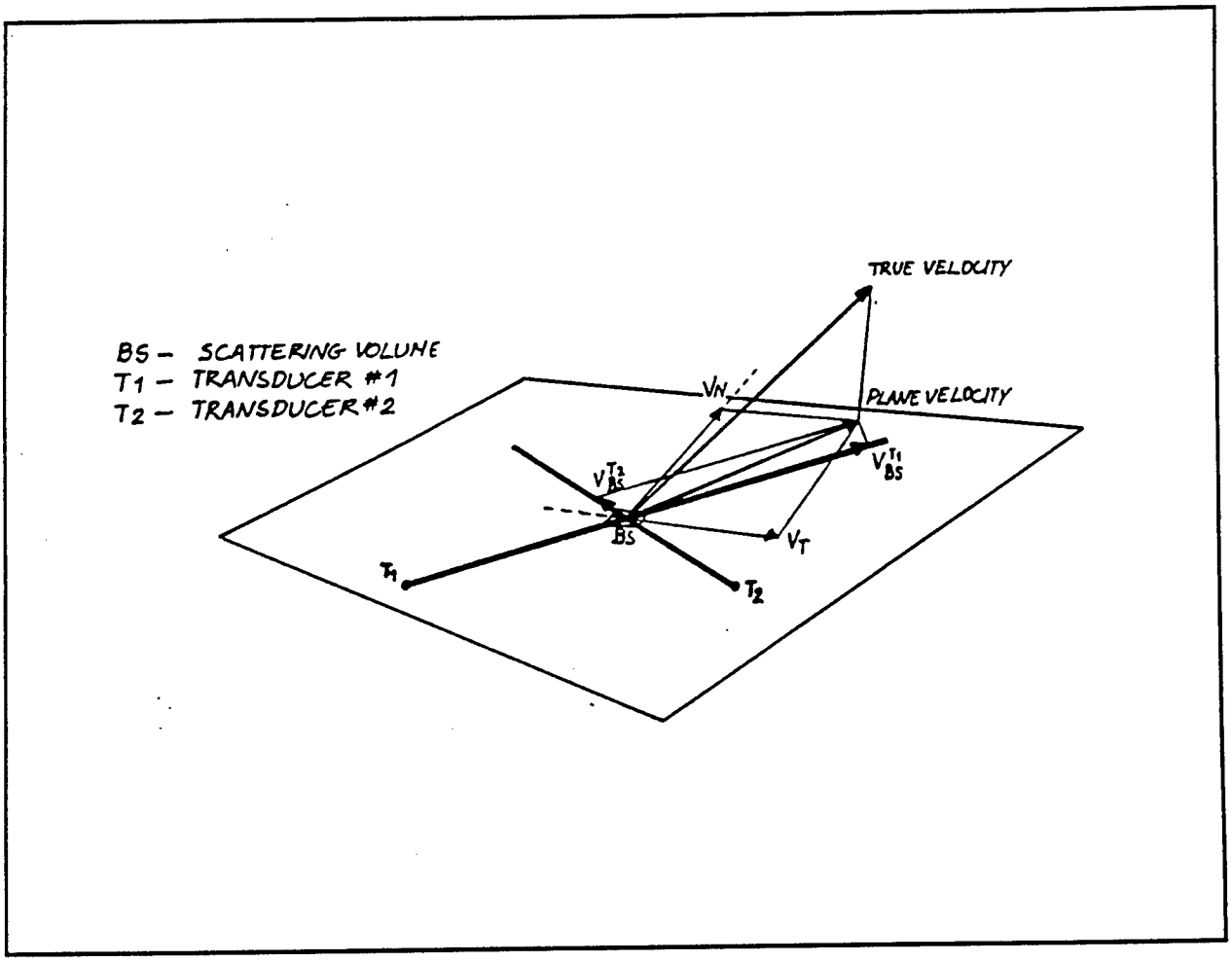

Figure 7. Schematic of the resolution of an arbitrary velocity vector in the bistatic mode of operation. T1 and T2 represent the location of two of the acoustic transducers, BS is the intersection point of the two narrow acoustic beams. An arbitrary true current velocity vector has been projected onto the plane formed by the T1 and T2 beam. The resolved component V_N (normal component) of the plane projected true velocity vector lies along the line bisecting beam directions from T1 and T2, while V_T (transverse component) is orthogonal to V_N. The component V_N is the doppler velocity detected by the bistatic pair T1 and T2.

relationships can be derived (for example Alonso and Finn, 1967). For a sound speed, c, a pulse transmitted at time t=0 will arrive at BS at time $t=t_1$, such that

$$c.t_1 = l + v_{BS}^{T1}.t_1 \Rightarrow t_1 = \frac{l}{c - v_{BS}^{T1}} \qquad (2)$$

where l is the path-length T1 - BS, and c is the sound speed of the medium. Now, if a second pulse is transmitted at time t_2, it will arrive at BS at time t_3 and, eliminating l

$$t_3 = \frac{l + c.t_2}{c - v_{BS}^{T1}} \Rightarrow t_3 - t_1 = \frac{c}{c - v_{BS}^{T1}}.t_2 \qquad (3)$$

If, during interval $(0,t_2)$ the transmitted frequency is f_{tx}, there will be $f_{tx}.t_2$ wave fronts arriving at BS, during the interval t_3-t_1. Therefore, the frequency detected at BS will be:

$$f_{BS}.(t_3 - t_1) = f_{tx}.t_2 \Rightarrow f_{BS} = \frac{c - v_{BS}^{T1}}{c}.f_{tx} \qquad (4)$$

The frequency f_{BS} is the frequency of the scattered signal at BS that is sent towards T2. Using the same procedure, the frequency measured at T2 can be derived:

$$f_{t2} = \frac{c}{c + v_{BS}^{T2}}.f_{BS} = \frac{c - v_{BS}^{T1}}{c + v_{BS}^{T2}}.f_{tx} \qquad (5)$$

If an arbitrary velocity vector at BS has a component V_N in the direction bisecting the angle formed by the two acoustic beams, (see Figure 7), then $v_{BS}^{T1} = -v_{BS}^{T2}$ and $f_{T2} = f_{tx}$. Therefore the only velocity component producing a doppler shift will be along the direction defined by the bisection of the two beams i.e. V_N. This component will have equal projections along the two beams, so that:

$$v_{BS}^{T1} = v_{BS}^{T2} = V^{12} = V_N \sin\theta \qquad (6)$$

Therefore

$$V^{12} = c.\frac{f_{tx} - f_{T2}}{f_{tx} + f_{T2}} = c.\frac{\Delta f^{12}}{2f_{tx} - \Delta f^{12}} \approx \frac{1}{2}.c.\frac{\Delta f_{12}}{f_{tx}} \qquad (7)$$

where the approximation is valid for low mach numbers ($V^{12} << c$), and so

$$V_N = \frac{1}{2\sin\theta}.c.\frac{\Delta f^{12}}{f_{tx}} \qquad (8)$$

Because of the symmetric geometry of this system, this expression is also true for the

case when T2 is transmitting and T1 receiving. This dual doppler frequency estimate creates redundancy in the observed doppler frequency, providing increased confidence of the estimates by averaging, and allowing the detection of inconsistent doppler frequencies which can arise from scatters near the edges of the acoustic sample volume. By having all three transducers transmit in sequence, three different slanted V_N velocity components are measured at the intersection volume.

The real-time doppler processing software, CASPHOST (see appendix B), estimates bistatic doppler velocities, backscatter amplitudes and doppler spectral widths at a 36 Hz rate using an AT&T DSP32C Digital Signal Processor (DSP) in the processing AT computer. These timeseries data are time-tagged and logged with the backscatter profiles every second to disk (see Appendix C for the data formats), and each variable may be interactively displayed as graphical timeseries in real time. A postprocessing software module, PostCASP, takes the slanted bisector doppler velocity components, applies weighted filtering to reject low amplitude or high spectral bandwidth doppler estimates, then resolves the slant doppler frequencies into an orthogonal frame in the instrument co-ordinate system, and optionally rotates the velocity vector into an earth-referenced level system by applying tilt sensor angles. A schematic of the coordinate system convention used for the CASP velocity data is shown in Appendix D.

4 Sediment Measurement Techniques

Suspended sediment concentrations are inferred from profiles of acoustic backscatter acoustic intensity by measuring the range-gated power returns from the 1.3 MHz transceiver and each of the 5.2 MHz transceivers. The backscatter power levels are converted to sediment concentration profiles using an acoustic model which includes the effects of attenuation due to water and suspended mass, and radial spreading, to produce profiles from 6 cm in front of the instrument head to the sediment bed, up to a range of 1.2 m. Under restricted conditions, the ratio of backscatter measured by the 1 and 5 MHz transceivers can be used to identify changes in the mean sediment size from the population the system has been calibrated with.

The theoretical and empirical basis for the relationship between concentration and acoustic intensity follows work by Libicki *et al* (1989), Hay and Burling (1982), and Hay (1991). For weak (single) scattering conditions, the response of a monostatic transceiver in the far field can be generally expressed as

$$\overline{V}=S\times\sqrt{\frac{M}{\rho_s}\times\frac{r_0}{r}\times F[n(a),f_\infty(ka)]}\times e^{-2\int_0^r \alpha_T dr}, \qquad (9)$$

where S is the transceiver system sensitivity, M is the mass concentration of sediment scatterers, ρ_s is the sediment density, r_0 is a reference range, and r is the range from the transducer, to compensate for the radial spreading of the signal. The response function F represents the acoustic response to an arbitrary sediment size spectrum, n(a), (where a is the scatterer radius), modelled by a far field acoustic form factor, f_∞(ka), (where k is the transmitted acoustic wavelength). The exponential term accounts for the along-beam attenuation of the medium, where α_T is the sum of the clear water attenuation, α_w, and the attenuation due to the presence of scatterers, α_s, integrated from the transducer face to the observation point at range r.

Hay (1991) and Hay and Sheng (1992) have explored both analytical and empirical physical acoustic models of the response function and form factor, extending analytical models for scattering from spherical solids to irregular sand grains through experimental backscatter measurements. The authors formulated a response function model assuming a unimodel, lognormal, sediment population which could be characterized by a mean grain diameter, a_0, and a distribution width, σ. The wavelength, k, and therefore frequency dependence of the form factor was exploited to estimate a_0 and σ using multiple frequency acoustic transceivers. Due to the very weak frequency dependence of backscatter levels to the width parameter σ, even with a three frequency sonar system, Hay and Sheng used an independently estimated σ value., but were able to estimate range-dependent changes in the sediment mean radius over several minute averages.

As evaluation of the acoustic system sensitivity, response function, F, and attenuation factor, α_s, from acoustic models all contribute significant errors, it was decided to base the mass concentration calibration of the CASP on direct laboratory measurements of the response of the system to known concentration of sediment sampled from the field site where the instrument is to be used. By using backscatter measurements at two well spread acoustic frequencies, departures from the sample mean diameter of the test sediment can be determined by this method. The model adopted for this method is given below, while the methodology for the calibration is given in section 5:

$$M(r)=V^2\times Calmass\times\frac{r^2}{r_0^2}\times e^{4\int_0^r(\alpha_w+\alpha_s(M))dr} \qquad (10)$$

where V^2 is the measured voltage output from the range-gated monostatic sonar, (or digital counts representing voltage), Calmass is the first order calibration coefficient determined from laboratory calibrations, r is the range from the transducer face to one of 68 range bins, and α_s (M)is directly estimated from laboratory measurements of signal attenuation in the sediment/water fluid, and, following Clay and Medwin, 1977 p98,

$$\alpha_w=3.52\ x\ 10^{-8}\ f^2+2.34\ x\ 10^{-6}\ S\ \frac{f^*f}{(f^2+f^{*2})}$$

where f = the transmitted frequency
S = the salinity in parts per thousand
f^* = 93200 Hz, the molecular relaxation frequency of $MgSO_4$.

As the sediment attenuation coefficient is a strong function of the sediment mass, a piece-wise method starting at the first range bin is used to evaluate the attenuation integral in equation (10), assuming that the previous bin is the best estimate for attenuation in the current bin. This evaluation of attenuation is critical to obtain meaningful concentration profiles at levels above 1 g/l for the 5.2 MHz sonars, and O(4 g/l) for the 1.3 MHz sonar. The laboratory measurements described in section 5 have further provided a method to audit the performance of this acoustic model, allowing limitations of the mass concentration model to be quantified.

The most significant limitation in using empirical calibrations based on actual sediment samples is that during actual field measurements, the sediment spectra may depart from the sample spectrum used in the calibration. However, as two frequencies are used, an estimate of the change in mean sediment radius may be made, assuming (just as the more elaborate acoustic models must) that the sediment population remains unimodel, lognormal, and with an unchanging lognormal width parameter. Clearly, significant departures from these

underlying assumptions in the acoustic models will give rise to serious errors, requiring *in situ* measurements of the sediment spectra, but at least the dual frequency response will allow these conditions to be identified. The overwhelming advantage for the direct laboratory calibration using actual sediment samples is that it represents a complete, end-to-end calibration of the system, with no *a priori* assumptions about the sediment spectra, and it provides robust calibration coefficients not only for the Calmass coefficient, but also for the important α_s (M) terms.

A potentially serious contamination of backscatter intensity can occur by the presence of air bubbles in the water column, particularly at frequencies below 200 KHz, due to the 10^2 to 10^6 greater acoustic cross section of resonant bubbles relative to their geometric cross section. The long residence time for very small bubbles is a potential problem for all non-invasive sediment measurements (including lasers) but their presence through the water column (in small to moderate concentrations) can be detected using a combination of acoustic frequency-dependant backscatter characteristics and optical backscatter levels. An MS thesis is currently investigating our ability to detect and correct for the presence of microbubbles using laboratory measurements and DUCK94 data. The CASP, as deployed in the DUCK94 experiment had a significant advantage by allowing it to be positioned close to the bed, minimizing the path-length between the sonar transceivers and the high-concentration bottom boundary layer. However, in the presence of strong wave breaking, our laboratory experiments have shown that both Optical Backscatter Sensors (OBS) and acoustic backscatter techniques can have significant errors in their estimates of sediment concentration.

The CASP acoustic front end electronics use a wide dynamic range, linear (constant gain) approach to minimize errors common in time varying gain circuits. System noise due to range binning, thermal noise, electronic noise sources and environmental noise all degrade the sensitivity and accuracy of sediment measurements. The requirements for low noise performance of the doppler velocity estimation described above have resulted in signal to noise ratios over 70 db in the CASP, providing a very wide sediment mass measurement, and corresponding wide range of doppler velocity detection. The complex amplitude homodyning receivers and signal processing estimation of power implemented for the CASP give a dynamic range and linearity at least an order of magnitude better than broadband rectified power circuits used by other investigators, significantly extending the lower threshold for sediment mass estimation. However, the doppler velocity estimation can be expected to "drop out" at very low backscatter levels, as the receiver signal to noise ratios fall below 10db (see appendix E). For typical conditions in the surf zone and muddy estuaries this is unlikely to be a problem, but for very clear conditions, a manual 20db gain selection has been implemented, but this high gain setting limits the highest resolved concentrations to approximately 10 g/l for the 1.3 MHz sonar.

5 Suspended Sediment Calibration

Laboratory Calibration Method

The work by others in calibrating the acoustic backscattered signal to estimate both the mass concentration and size of sediment is borrowed upon and expanded. A widely used procedure (see for example Young *et al*, 1982; Tamura and Hanes,1986) has been to calibrate the instrument as a function of concentration by creating a suspension along the entire acoustic path over a distance typically used in the field (~1m). Bottom sediments from a particular field site are used in the calibration. A difficulty of this approach is that it requires that attenuation due to particles in suspension along the sound path be compensated, which is particularly challenging in the complicated near field of the acoustic transducers.

More recently, Hay (1991) used a turbulent jet to maintain a statistically steady suspension localized along the sound path. This makes it possible to confine the scatterers to the transducer far field and to conveniently measure the attenuation of the incident sound passing through the jet. The suspended sediment load of the jet was measured independently by drawing samples by suction through a J tube oriented into the flow. For the suspended sediment sample to be representative, the sampling must meet the following criteria: 1) the suction velocity must be great enough (greater than 1 m/s in this case) to avoid particle settling problems in the suction line, 2) that the suction velocity be comparable to or greater than the speed of the external stream, and 3) the intake is oriented into the flow.

Another technique described by Lowe et al (1991) is to calibrate grain concentration and velocity by suspending sands in aqueous solution of high viscosity glycerol, and towing the sensor over the stationary suspensions at known speeds.

A new approach has been taken to incorporate the calibration of the transducer beam responses and sediment concentration response for the CASP. A test tank has been constructed using a 600 gallon acrylic aquarium equipped with a computer-controlled X/Y positioning stage, from which the CASP is suspended (see photograph in Figure 8). Targets can easily be suspended in front of the probe while the instrument is moved in small increments in X/Y space to determine, for example, the angular sensitivity of the acoustic transducers and the precise intersection point of the beams. This usually laborious task is simply handled by the data acquisition computer which sends position commands to the intelligent servo controller, acquires and averages the specified acoustic data, then moves to the next position in the measurement loop.

An internal test vessel is used within the test tank to calibrate acoustic backscatter levels against known sediment concentrations. A schematic of the sediment test vessel is shown in Figure 9, and can be seen in the right hand side of the photograph in Figure 10. The CASP acoustic beams are directed through an acoustically transparent window in the side of

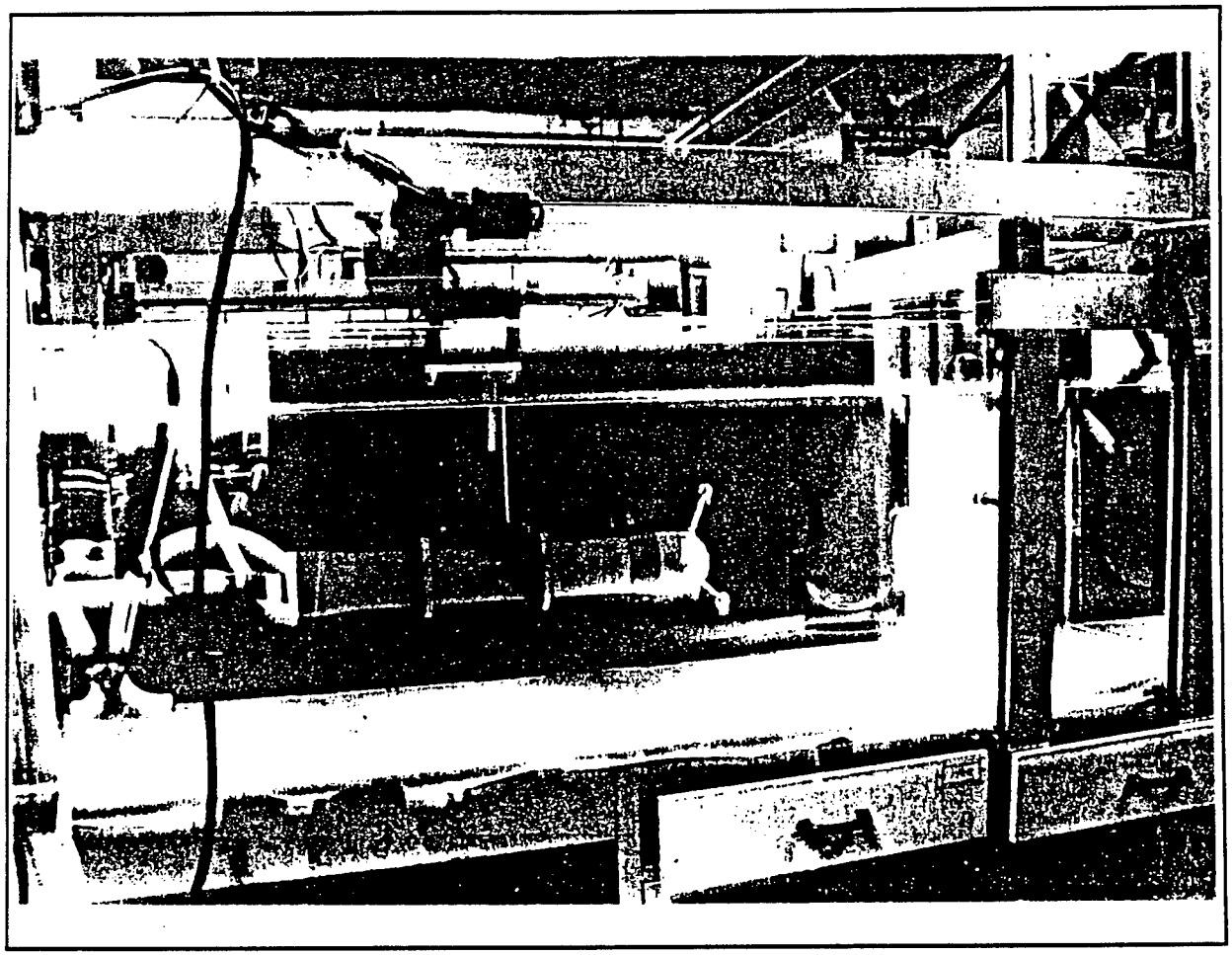

Figure 8. Photograph of the test and calibration tank. The servo-controlled instrument stage can be seen above the 600 gallon acrylic tank, supporting the CASP probe. The X/Y stage can move the CASP 80cm along the tank and 50cm across the tank. The brightly lit acrylic sediment vessel is in the right hand end of the tank.

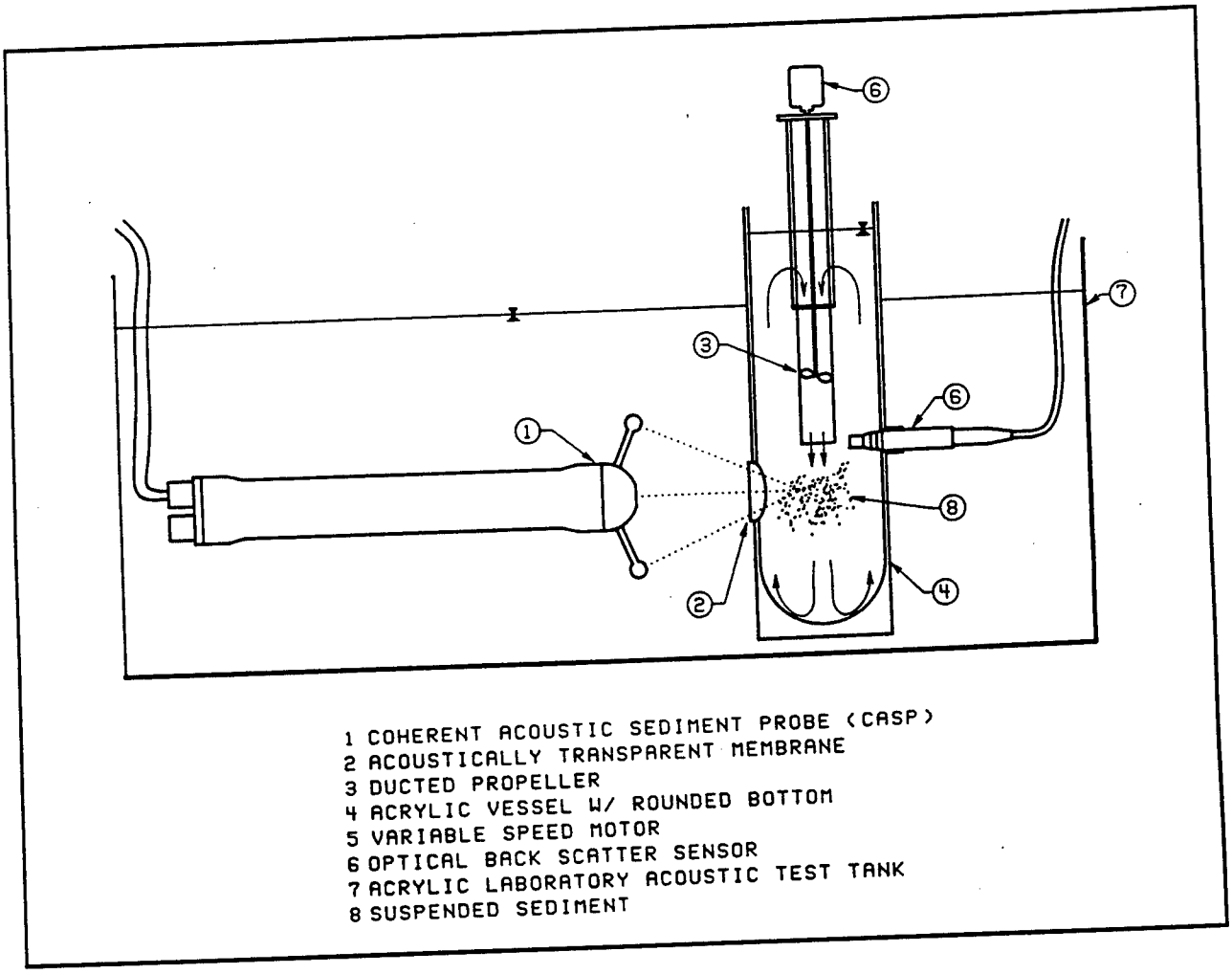

Figure 9. Schematic of the test tank and mixed sediment test vessel. While the CASP and test vessel sit within the larger tank, measured amounts of sediment are introduced into the fixed volume test vessel. A strong impeller pump and curved tank base keep the sediment in suspension while the CASP acoustic backscatter intensity measurements and optical backscatter sensor (OBS) data are logged.

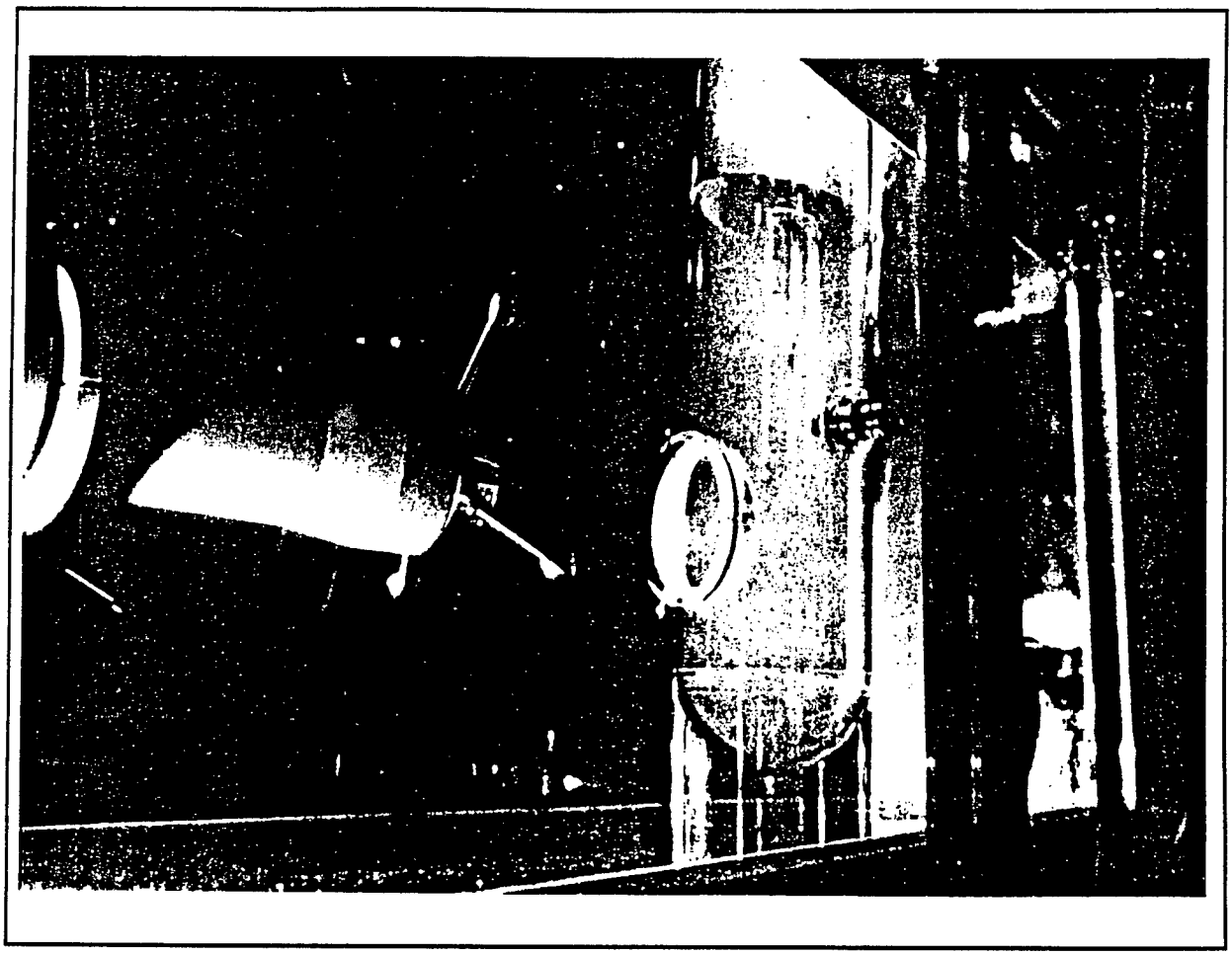

Figure 10. Photograph of the CASP and sediment test vessel. The CASP (left hand side) is directed into the test vessel through an acoustically transparent window into the well mixed sediment suspension in the test volume.

the acrylic test vessel which contains water and carefully measured masses of test sediment. A strong impeller-driven pump rapidly circulates the fluid and sediment within the measured volume of the vessel, creating a well homogenized volume with known concentration. The test vessel has been carefully designed to eliminate any level surfaces or flow stagnation points which might locally hold part of the sediment mass. Turbulence levels and recirculating flow speeds are maintained at sufficiently high levels to mix sediment particle sizes up to 2.2 mm at concentrations up to 100 g/l without entraining bubbles into the volume. As the test volume and sediment mass are known, the backscatter level to concentration relationship for all the beams can be readily determined by taking O(100 s) averages of the received intensities. The effects of the clear-water (main tank) attenuation and absorption by the acoustic window are taken into account in the absolute calibrations.

Sediment mass concentration and attenuation calibrations were made by recording continuous timeseries of the CASP data stream (which includes two OBS sensors in the sediment tank) from completely clear, unstirred conditions, to well stirred conditions while incremental measured masses of sample sediment were added to the test volume. Typically 3 minute periods are used between successive sediment increments to allow robust estimates of backscatter intensity to be obtained, and average out high frequency turbulent fluctuations in the stirred test vessel. The dry weighed samples were wetted in a weak Triton 100 solution several hours before being introduced into the test vessel to minimize the effects of micro-airpockets being trapped on the grain surfaces. The time-tagged data stream was then processed through our standard processing chain to produce temporal averaged profiles of backscatter power in units of raw counts squared (1 volt = 3276 counts).

The following sections report the acoustic beam characteristics which define the sample volume in the range-gated sonar system, then show backscatter calibrations for sediments sampled from the trough at FRF, Duck North Carolina during the August 1994 DUCK94 experiment.

Acoustic Beam Characteristics

The diameter of the flat, circular piston transducers used in the CASP were selected to have comparable farfield directivity functions so they defined comparable sample volumes at large ranges. The directivity is given by

$$D(\beta)=\frac{2J_1(k_c a_0 \sin\beta)}{k_c a_0 \sin\beta} \qquad (12)$$

where J_1 is the cylindrical Bessel function of order 1, and k_c ($=2\pi\lambda$) is the transmitted wavenumber. The nominal range bin size, defined by the transmitted pulse length, bandwidth of the receiver and sample interval is 1.7 cm for all four beams. Each of the four beams has 68 range bins of data distributed in sub-frames of two 1.68 cm bins followed by a 3.360 cm

bin, repeated over a 1.16 m maximum profile length.

As the two dimensional directivity function of piston transducer becomes highly structured in the near-field, where the many simultaneously driven piston pressure sources across the transducer face interfere strongly, it is highly desirable to make backscatter measurements outside this region. The nearfield range is conservatively defined by $r > \pi\ a_0^2\ \lambda$, although average response errors are small for ranges as close to 1/3 of this range, as can be seen in the relatively smooth cross beam response function seen in Figure 11. The following table summarizes the theoretical far-field ranges, half-power beamwidths and nominal range bin length for the CASP.

TABLE I CASP MONOSTATIC ACOUSTIC BEAM CHARACTERISTICS

Frequency (MHz)	Transducer Radius (cm)	Wavelength (cm)	Farfield Range (cm)	Half Power Beamwidth (deg)	Half Power Beamwidth (cm)	Pulse Length (cm)
1.323	1.27	0.112	45.2	2.62	1.14	1.68
5.292	0.217	0.028	11.3	2.62	1.14	1.68

As a number of factors can degrade the transducer response and introduces spurious sidelobe responses to any physically realizable transducer system, the shape of the ensonified volumes were determined by measuring the actual received/processed acoustic power as the CASP instrument was moved by the computer-controlled x/y stage past a vertically orientated 50 micron stainless-steel wire. Figure 11 and 12 show the two dimensional response pattern for the 1.3 MHz and one of the 5.2MHz sonars respectively at a range of 25cm. For this calibration, the y grid axis represents the cross beam direction, while the x axis is along the beam. The upper panels show the equivalent Analogue to Digital Convertor (ADC) counts (where 32768 counts = 10 volts), while the lower panel shows the $\log_{10}$ received power (expressed as counts^2), emphasizing the 7 orders of magnitude dynamic range of the power measurements, and low magnitude sidelobe response of the transducers (which are consistent with theoretical predictions of equation (12)). This ensures that the sample volume is well defined, and that there is minimal response from strong scatters off the beam axis. The beam responses measured using four different wire diameters are summarized in table 2.

TABLE 2 β_m ANGLE OF THE FIRST NULL RESPONSE MINIMUM

Frequency (MHz)	50 micron wire	80 micron wire	100 micron wire	128 micron wire	$<\beta_m>$
1.323	2.04	2.66	2.66	2.66	2.51
5.292	2.86	2.86	2.86	2.65	2.81

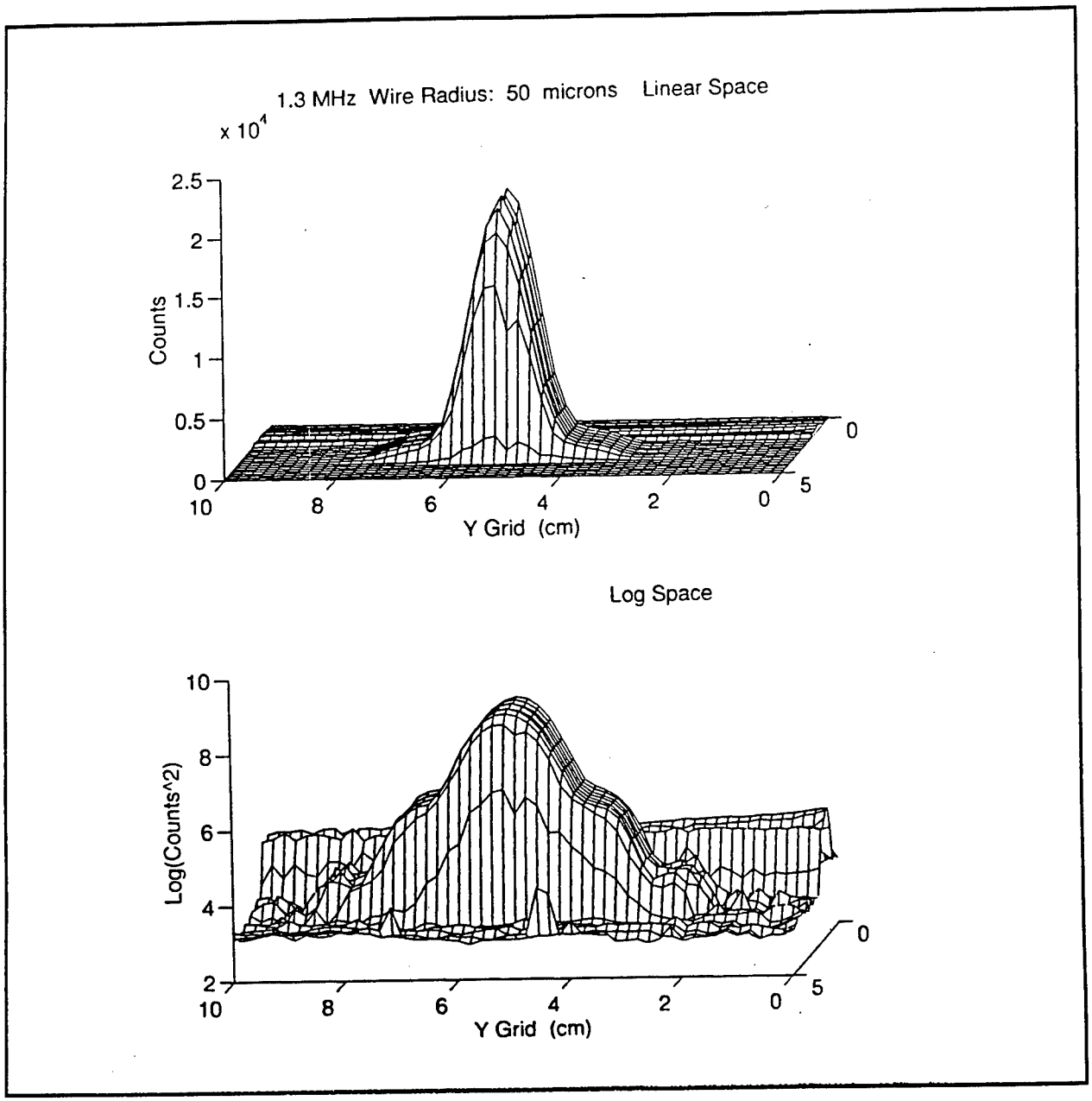

Figure 11a. Received acoustic pressure amplitude for beam 1 (1.3 MHz) in units of ADC counts as the CASP scans across a 50 micron stainless steel wire suspended 25 cm from the instrument head. The CASP was programmed to move 10cm across the beam axis and 5 cm along the beam axis. 11b. $\log_{10}$ of the received acoustic power for the same sample grid as panel a. The vertical power axis covers 8 orders of magnitude, and a weak multiple reflection from the back of the tank can be seen near x =1.

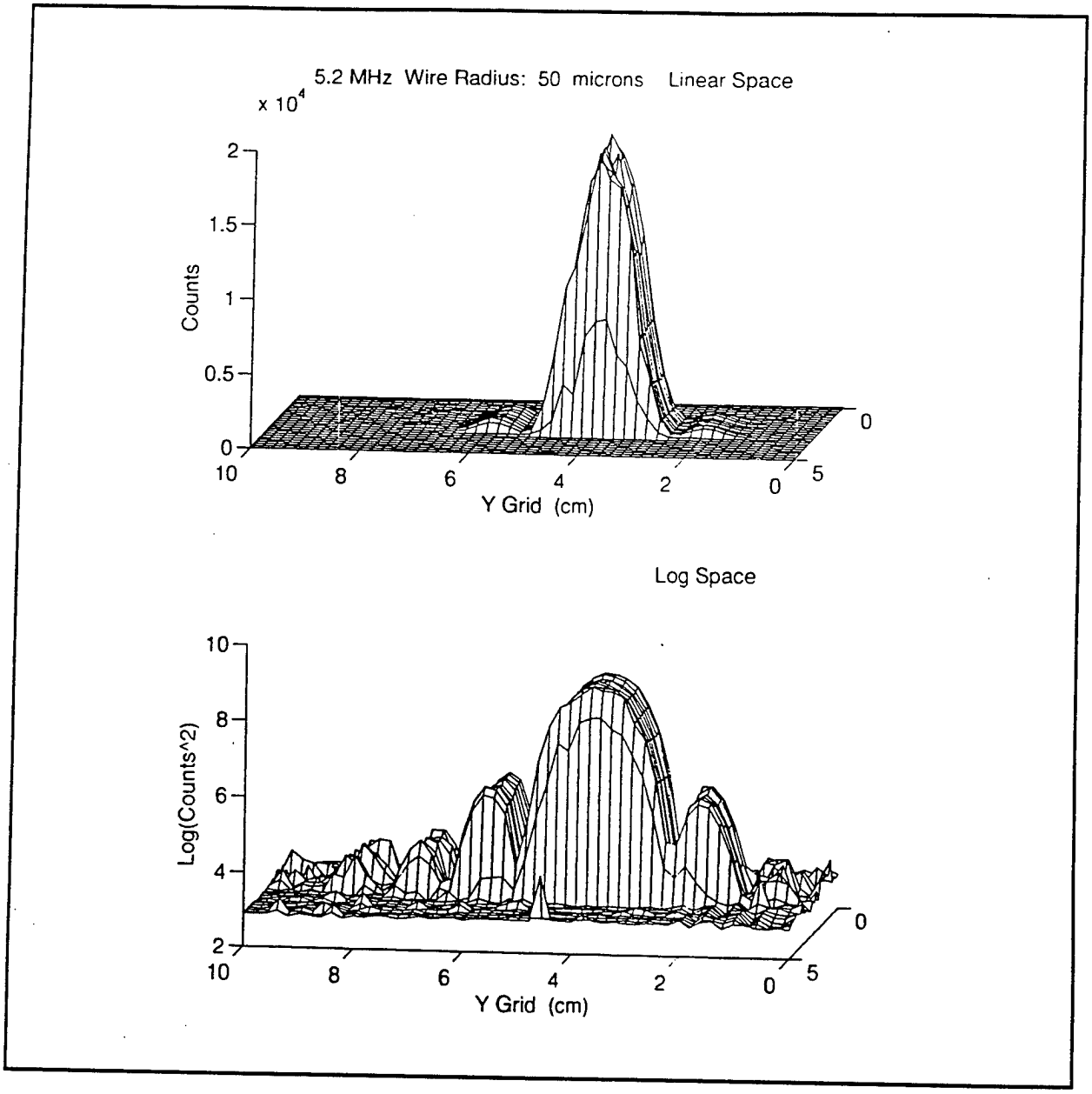

Figure 12a. Received acoustic pressure amplitude for beam 2 (5.2 MHz) in units of ADC counts as the CASP scans across a 50 micron stainless steel wire suspended 25 cm from the instrument head. The CASP was programmed to move 10cm across the beam axis and 5 cm along the beam axis. 12b. $\log_{10}$ of the received acoustic power for the same sample grid as panel a. The vertical power axis covers 8 orders of magnitude.

Attenuation Coefficient Calibrations

In the following two sections, calibration data is shown for sediments sampled from the trough at FRF, Duck North Carolina during the August 1994 DUCK94 experiment. The nominal size distribution for the sample is shown in Figure 13, with lognormal fitting parameters of a_0 = 120 μm, and σ=1.3.

During tank calibrations, the CASP is positioned such that the beam intersection point is approximately 3 cm inside the thin plastic membrane window which confines the high sediment volume in the stirred test vessel. The attenuation is estimated by a linear fit to the exponential decay of the signal response across the sample volume, with the radial spreading term removed, expressed by

$$\alpha_s(M) = \frac{\ln\left(\frac{r}{r_0}\frac{C(r)}{C_0}\right)}{-2\Delta r} - \alpha_w \qquad (13)$$

where r_0 is a reference bin within the sediment/water sample volume (clear of the acoustic window), Δr is the range bin size, C_0 is the receiver output (in digital count units) at the reference range r_0, and the clear water attenuation coefficient is evaluated using Equation (11). The linear fit between α_s (M) and the calibration mass concentration, M, provides a calibration factor, aslope. Figure 14a,b,c and d show these regressions for the four beams, over a concentration range of 20 g / l for the 1.3 MHz sonar (transducer 1), and 8 g/l for the three 5.2 MHz beams (2, 3 and 4). As the attenuation should be independent of any properties of the physical acoustic system, (but rather is a property of the scattering cross-section of the sediments at a given frequency), the three aslope estimates for the 5.2 MHz sonars are the same. For the Duck94 sediment sample, aslope = -0.0857 $m^{-1}/(g/l)$ has been used for the 1.3 MHz sonar, and aslope = -1.05 $m^{-1}/(g/l)$ for the three 5.2 MHz sonars. The limits of validity for these attenuation coefficients are 10 g/l for the 5 MHz sonars, and 100 g/l for the 1.3 MHz sonar. Beyond these concentrations the linear relationship with increasing mass breaks down as strong (multiple) scattering effects begin to dominate, and the acoustic model underlying Equations (9) and (10) is no longer valid. The strong departure from the linear dependency can be seen clearly as the attenuation - mass relationship flattens at 10 g/l concentration for the 5.2 MHz sonars, (Figure 15b), while the 1.3 MHz points (Figure 15a) remains essentially linear over the full calibration range.

Sediment Mass Calibration

Calibrations of sediment mass are based on the backscatter power levels (expressed as

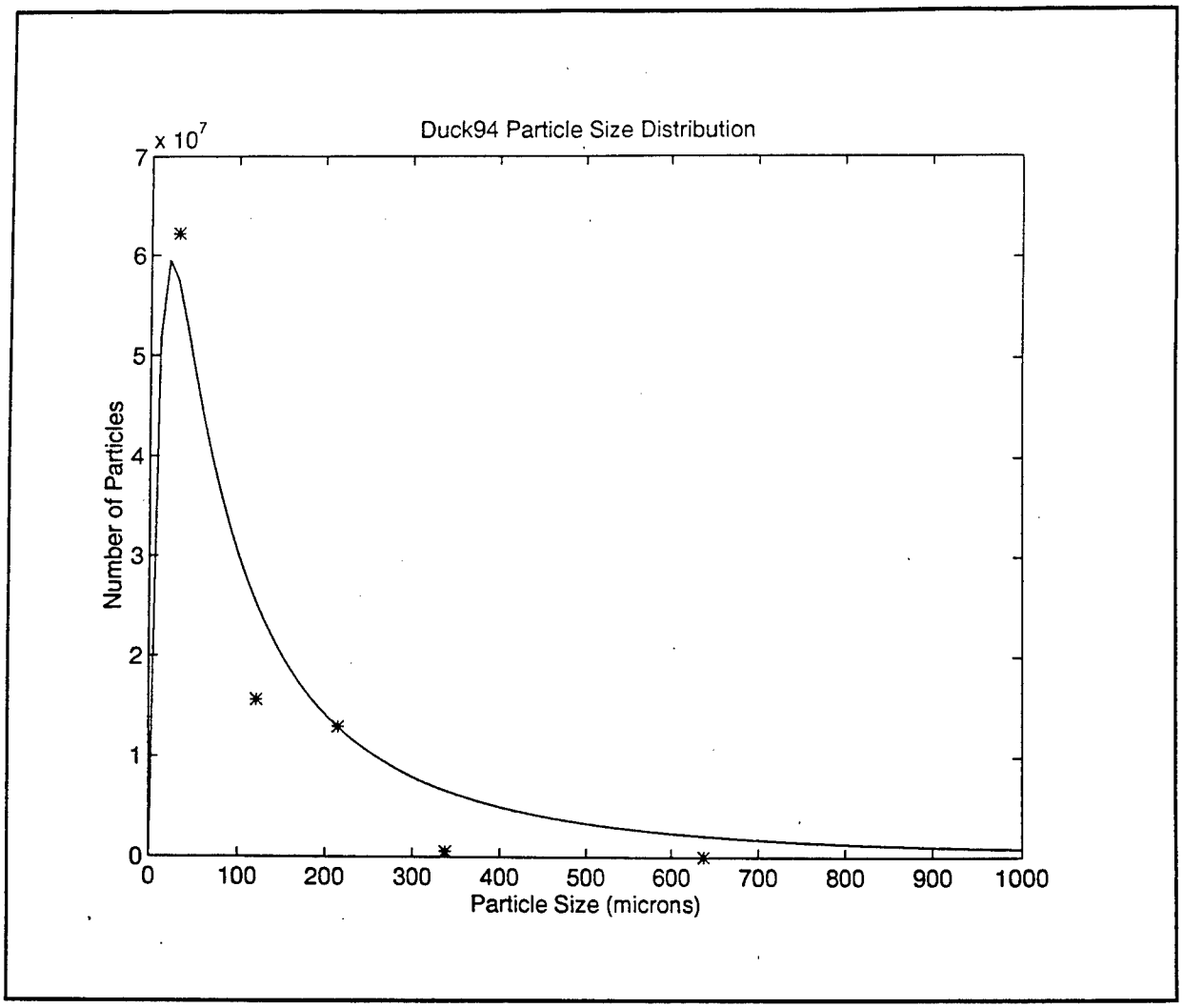

Figure 13. A size spectrum for the sediment sampled used in the CASP calibrations, based on sifted samples of 200g of sediment. The lognormal fit to this distribution is shown with a geometric mean particle radius of 120 microns and width parameter σ = 1.3.

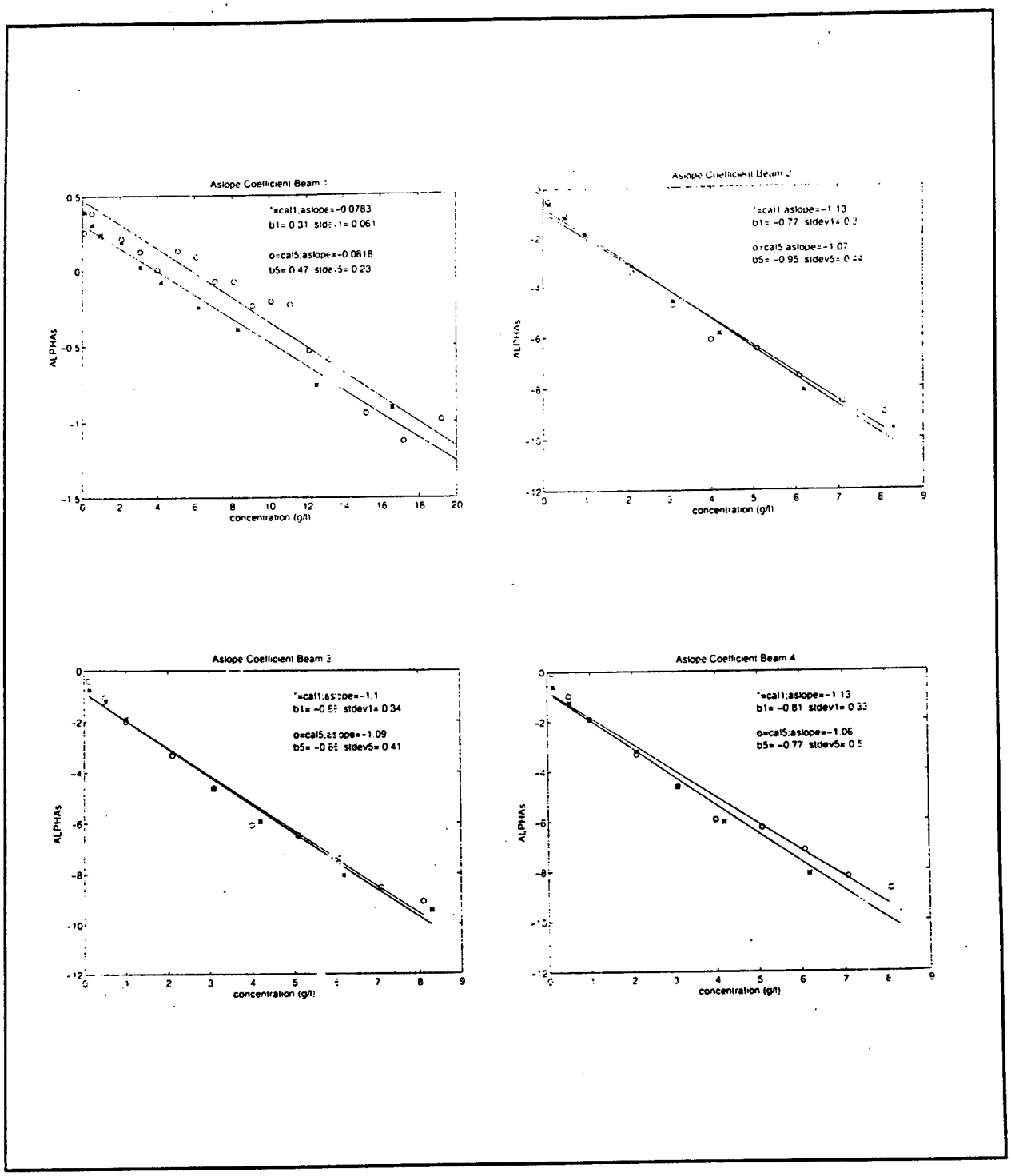

Figure 14 a - d. The estimates of α_s for acoustic beams 1 to 4 respectively. The ○ and * symbols are for two different calibration runs.

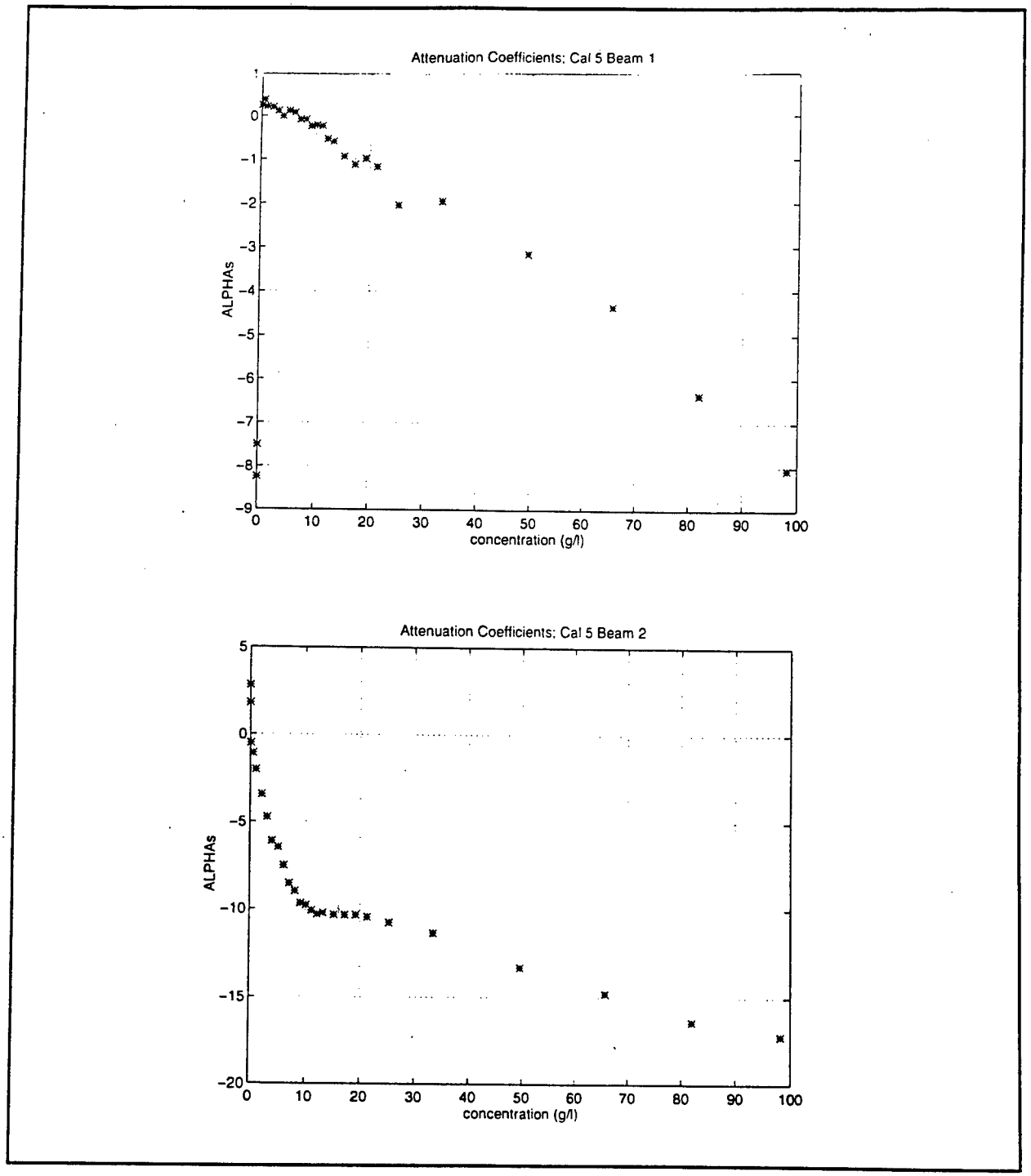

Figure 15 a. The estimates of α_s *vs.* mass concentration for beam1 (1.3 MHz). 15 b. The estimates of α_s *vs.* mass concentration for beam2 (5.2 MHz) showing the rapid departure from a linear relationship at concentrations above 10 g/l.

counts^2) within the stirred test volume containing known mass concentrations of the sediment sample. However if attenuation due to the presence of scatterers is not accounted for, robust estimates cannot be made. This is illustrated in the Figure 16, where the backscatter power is plotted against the range bin number at four different high concentration levels from 21 to 50 g/l. The test volume containing the sediment starts at bin 12, and the back of the test volume is atbin 20. The effects of strong attenuation can clearly be seen by the rapid exponential decay in power measured by the sonar receiver, indicated by circles, across the test volume. (This exponential decay is fitted to estimate α_s). However, to estimate the relationship between received power and mass concentration, the attenuation effects are removed by applying the range-dependent radial spreading and integrated attenuation factors across the sample volume:

$$V(r)_{comp} = V(r) \frac{r_0}{r} e^{-2\int_0^r (\alpha_w + \alpha_s(M))\, dr} \qquad (14)$$

The resulting power vs. range responses are shown as * symbols in Figure 16, and clearly linearize the backscatter power across the constant concentration test volume.

With these range-dependent terms accounted for, typical regressions of received power vs. M for a calibration run are shown for the four acoustic beams in Figure 17 a,b,c,d. In each of these plots, the raw received power from bin 13 (the first range bin completely inside the sediment test volume) is shown as * symbols, the symbols have the attenuation and spreading compensation of equation (14). applied, and the + symbols represent the mean compensated power for all the valid bins across the test volume. The latter data points are used to determine the calmass coefficient to scale received power (in counts^2) to mass concentration (g/l). For the Duck94 sediment sample, the following mass calibration coefficients were derived:

Beam1, 1.3 MHz : calmass = 3.79 * 10^{-8} (g/l) / counts^2
Beam2, 5.2 MHz : calmass = 2.05 * 10^{-8} (g/l) / counts^2
Beam3, 5.2 MHz : calmass = 2.27 * 10^{-8} (g/l) / counts^2
Beam4, 5.2 MHz : calmass = 2.53 * 10^{-8} (g/l) / counts^2

Differences in these coefficients arise from small differences in the transducer and front-end electronic sensitivities, which are accounted for in this end to end calibration method.

Field backscatter power measurements are converted to estimates of sediment profiles by applying these laboratory-derived coefficients to Equation (10). As the sediment attenuation coefficient, α_s, is dependent on the mass concentration, this equation does not have an explicit solution, so a two-pass iteration is used. In the initial solution of $M_i(r)$, the attenuation integral is piecewise evaluated starting at bin 5 (to avoid near-field problems and transducer ringing) by using the mass estimates from the previous bin, to evaluate α_s for the current bin.

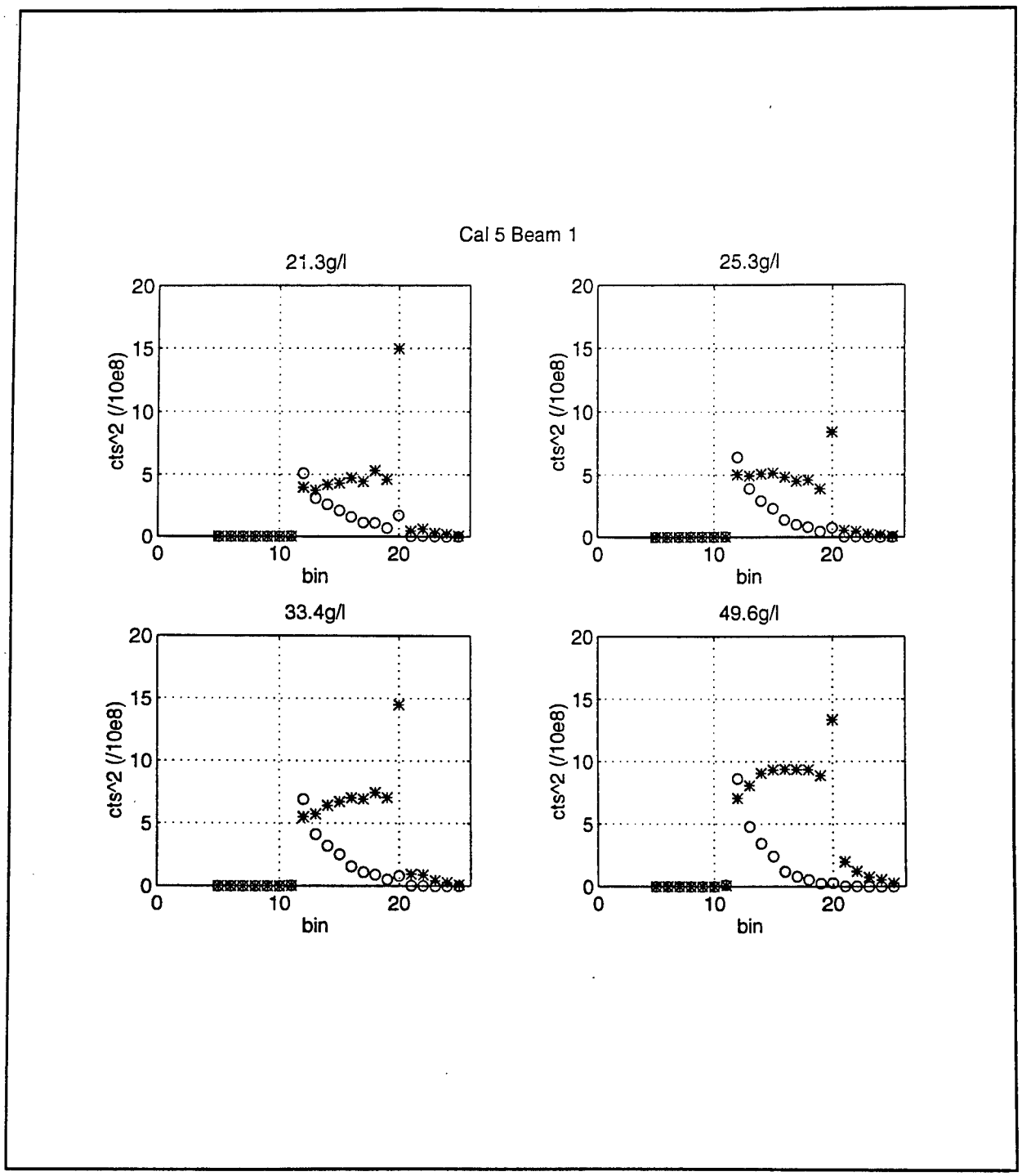

Figure 16 a - d. The received acoustic power *vs.* range bin at concentrations 21.3, 25.3, 33.4 and 50 g/l. The ○ symbols show the raw received power, and the * symbols indicate the power after compensation for radial spreading and attenuation.

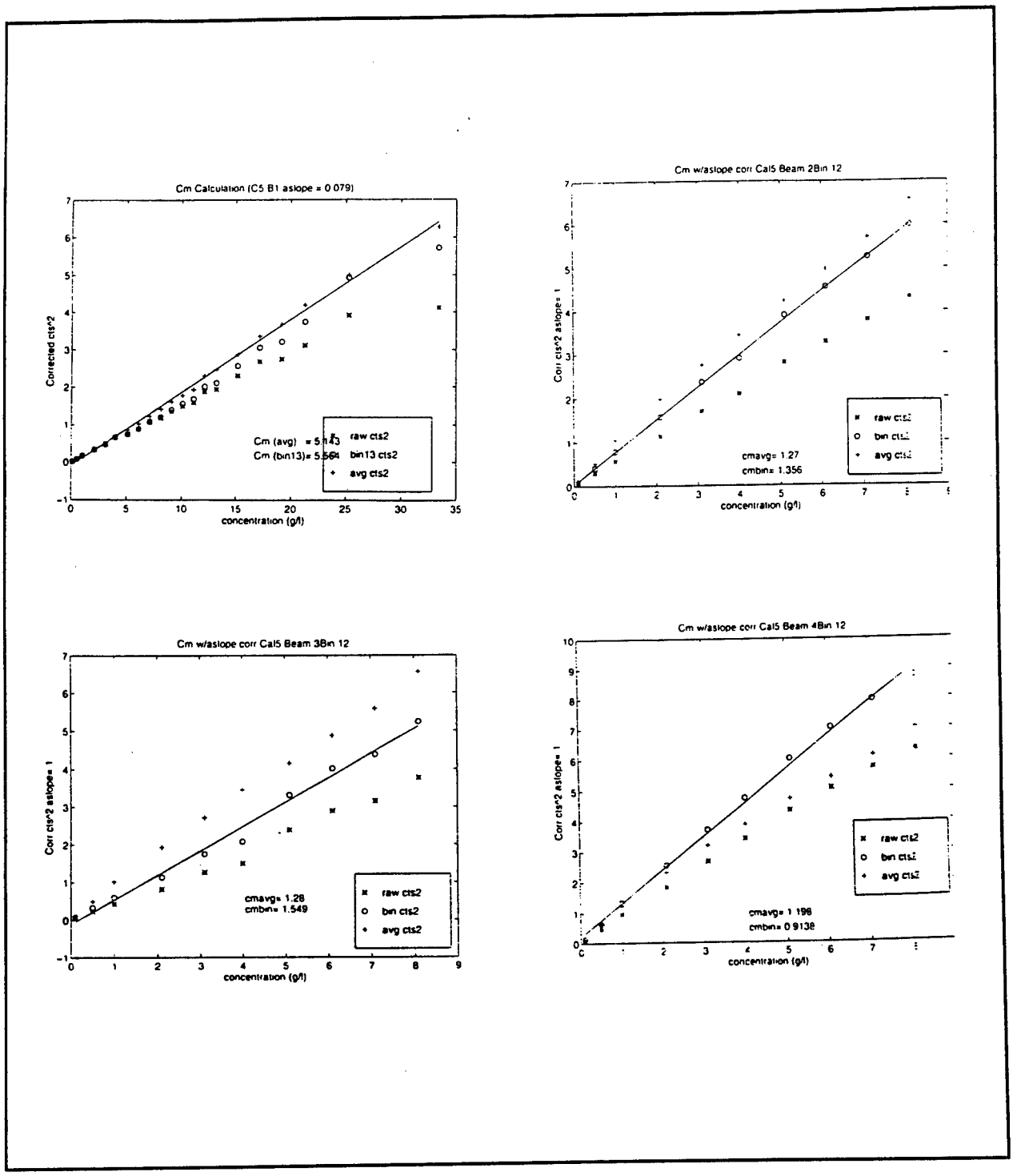

Figure 17 a-d. Corrected received power *va.* mass concentration for beams 1 - 4. The * symbols indicate the uncorrected power for bin 13 (the first range bin inside the sediment test vessel), the o symbol is the corrected power for bin 13, and the + symbols indicate the average over all the valid range bins within the test vessel.

In the final pass, these initial mass estimates, $M_i(r)$, are used in the piecewise integral to improve the mass concentration estimates, particularly in high vertical gradient conditions.

An illustration of the ability of this algorithm to work over a wide range of concentration values is shown in Figures 18 a - d, where the estimated concentration is plotted against the actual concentration over range bins 10 to 18. The start of the test vessel is at bin 12, with the very clear water in the main tank seen by bins 10 and 11. These surfaces clearly show the validity of the acoustic model and its implementation to estimate mass concentration over a very wide range. Without the attenuation terms, the errors across the test volume (high bin numbers) would exceed 300% for the 1.3 MHz sonar at 35 g/l, and 800% for the 5.2 MHz sonars at 10 g/l. Even with the algorithm carefully applied, the more distant range bins of the 5.2 MHz sonars show >20% underestimates of concentration. Therefore, for this sediment population (which is typical of open ocean surf beaches in the surf zone), the 1.3 MHz sonar is usually used as the primary measurement of sediment concentration. It should be emphasized that this integration is subject to significant errors if the mass estimates are in error in previous bins, so the backscatter estimates have to be robust representations of the actual mass profiles. For most boundary layer problems, this sensitivity is usually mitigated by the strong increase of suspended mass with range. In the Duck94 data described in section 6, the mass profiles were successfully determined with temporal resolutions of 4 Hz.

Sediment Size Discrimination

As two different frequencies are used in the CASP, it is possible to exploit difference in magnitude of the response function, F (see equation (9). above) to different wavelength (and hence frequency) acoustic waves as properties of the scattering population change. For sediments which can be characterized by a lognormal distribution with a fixed distribution width, for example, the difference in response of the 1.3 and 5.2 MHz sonars can be modelled. Following the development of Hay and Sheng (1992), the response functions for the two CASP sonar frequencies are plotted in Figure 19 a and b as a function of mean geometric radius of sediment particles up to 200 microns, over a range of σ from 1.1 to 1.5 (where σ is the lognormal distribution width parameter). These functions show the weak dependence of the sonar power response to large differences in distribution width, which forced Hay and Sheng to fix σ in their multifrequency sonars.

However a significant difference in response at the two frequencies does occur, particularly as the sediment distribution tends to smaller mean radii. The ratio F_5/F_1 shown in Figure 20 illustrates this relationship, providing a means of determining changes in mean sediment size from the backscatter profile data. This sediment sizing method has been implemented in the CASP processing by calculating the apparent mass measured at the wo sonar frequencies, and using their ratio to indicate changes in mean sediment size. Several cautions must be stated in using this size discriminator:

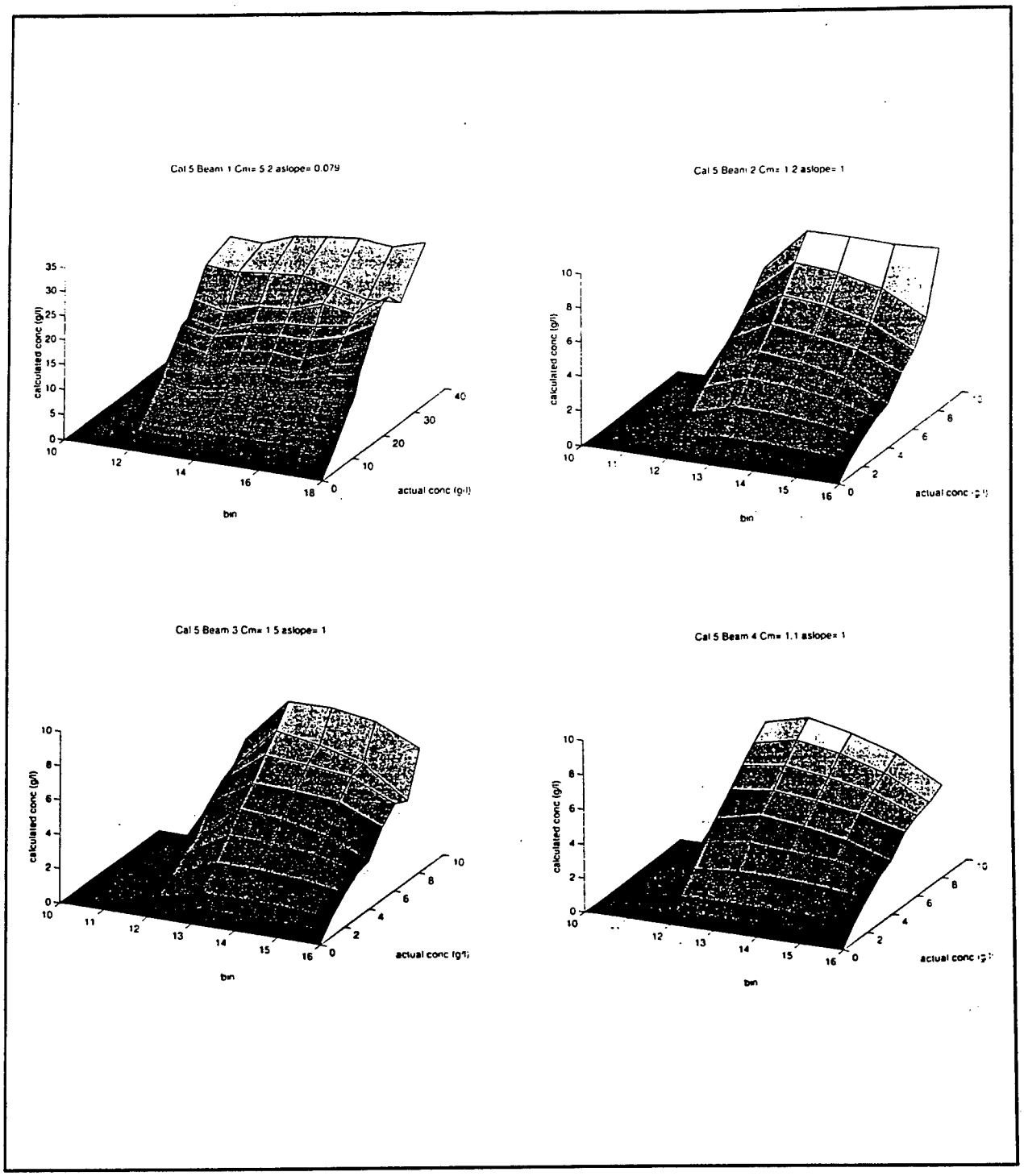

Figure 18 a- d. Estimated mass concentration *vs.* actual mass concentration over range bins spanning the test vessel for beams 1 - 4. Bins 10 and 11 are outside the sediment test vessel.

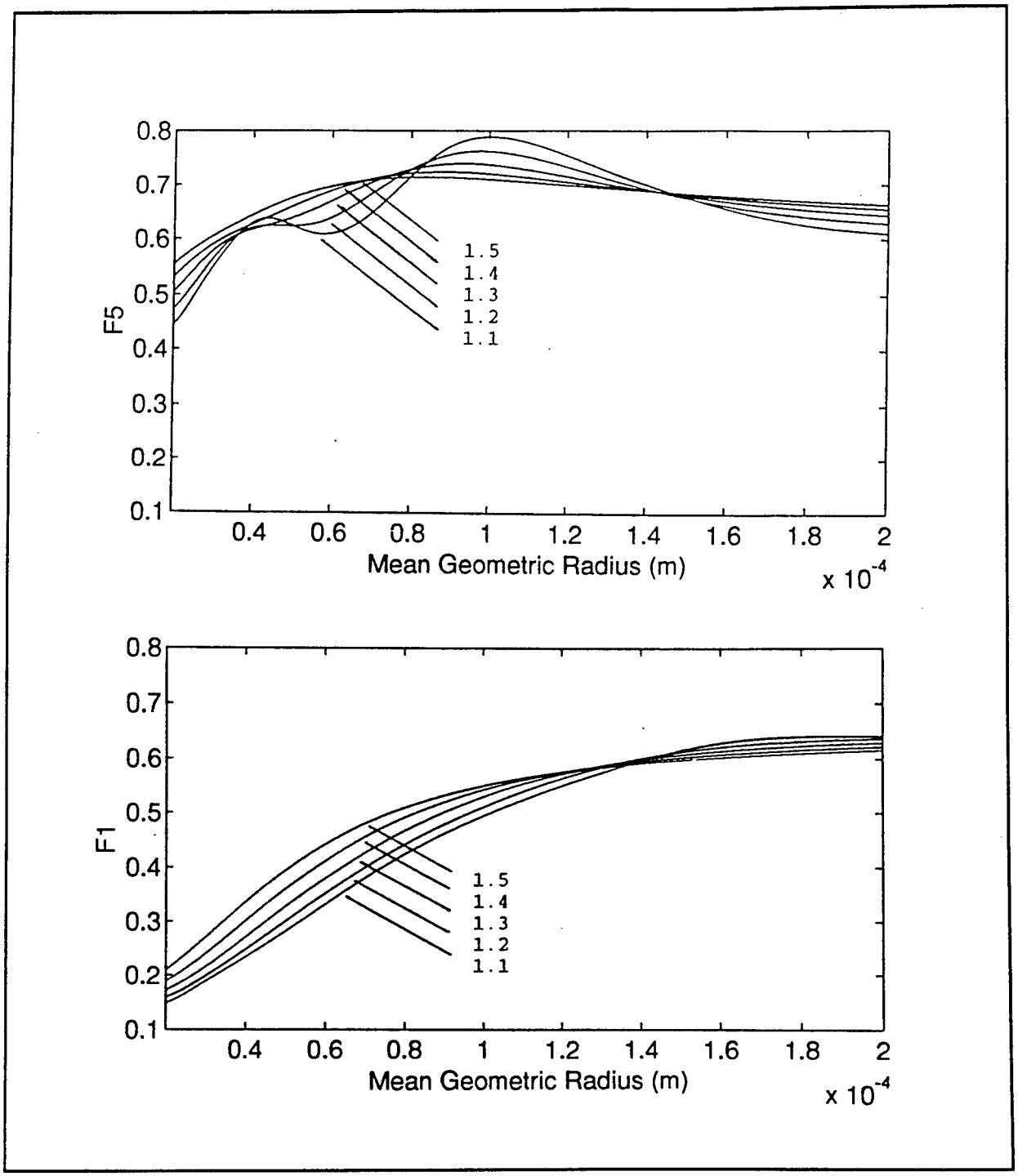

Figure 19a and b. The response function based on a lognormal distribution of quartz sediments for the 5.2 and 1.3 MHz sonars respectively. The response functions are plotted as a function of geometric mean diameter of the lognormal distribution for width parameters between 1.1 and 1.5.

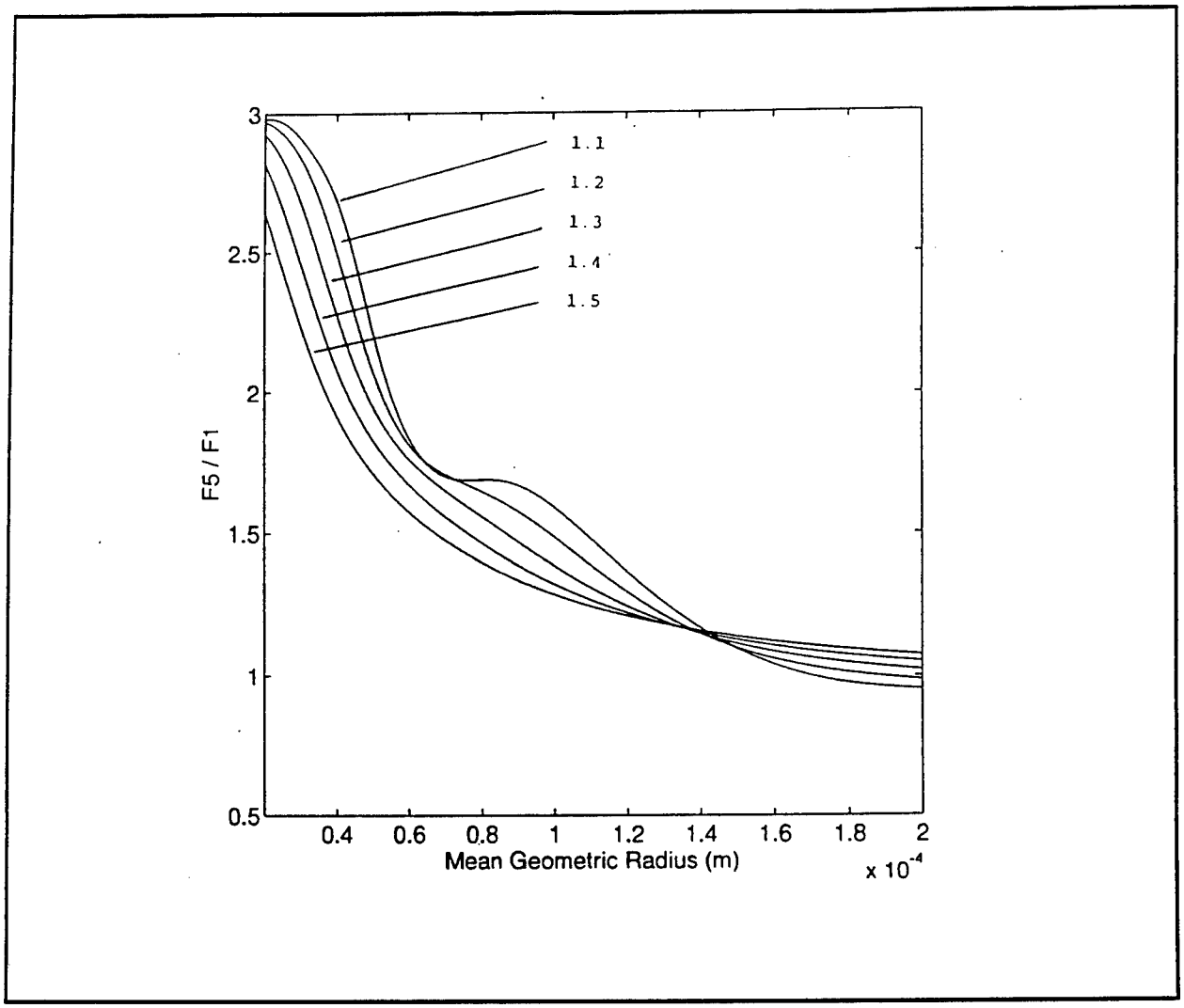

Figure 20. The ratio of the 5.2 to 1.3 MHz response functions *vs.* geometric mean sediment radius for lognormal width parameter values from 1.1 to 1.5.

1.) The apparent concentration profiles have to be determined to O(10%), suggesting that longer averaging intervals need to be used than the default 4 Hz profiling rate.
2.) Large departures in sediment size from the sediment population used to calibrate the system will result in invalid M(r) estimates (equation (9)) as the calmass and aslope coefficients will no longer necessarily be valid.
3.) As the 5 MHz sonars only give reliable results to concentrations of 10 g/l, this puts an upper bound on the range of interpreting the response function ratios. i.e. if the mass estimated by the 1.3MHz sonar is greater than 10 g/l, the size discriminator returns null values.
4.) The shape of the F_5/F_1 curves in Figure 17 shows that there is very poor size discrimination as mean radius increases beyond 120 microns.

These cautions emphasize the limited applicability of size discrimination inherent in multifrequency (and particularly dual frequency) acoustic systems, but the response function ratio still provides a useful diagnostic in determining mean size changes.

6 CASP Field Measurements From DUCK94

During Duck94, the CASP was deployed from an instrumented sled which made cross-shore transects from the shore-ward side of the bar to the beach face over the course of each day of the experiment. The CASP was mounted on a hydraulically actuated space frame which allowed it to be raised and lowered remotely during each O(1 hour) measurement station. Typically the CASP primary sample volume (25 cm in front of the instrument head) was vertically positioned to profile the three component velocity vector at 4-8 levels from the sediment bed to approximately 60 cm above the bed. Continuous backscatter profiles were measured at each measurement height, allowing the temporal changes in sediment mass profiles to be estimated concurrently with three component sediment fluxes.

A short example of the CASP data is shown here to illustrate the performance of the CASP in field conditions. The 100 second timeseries sample is taken from day 20, where 2 m significant wave height, narrow-banded swell was shoaling across the bar and trough. The sled was positioned just inshore of the center of the trough (187 m from the shore datum) during this station. Figure 21 shows a 100 second timeseries of the three velocity components measured 1.5 cm above the bed, with u the cross-shore, and v the offshore velocity components. This 36 Hz sampled data shows high level turbulent fluctuations in all three components and periodic, highly skewed cross-shore velocity spikes as the very non-linear, shoaled swell traverses the trough. The resulting Reynolds stress vectors $(u'w' + \mathbf{i}\, v'w')(t)$ are in Figure 22a, and the 36 Hz shear velocity estimates (u_*) are in panel b, with a 1 second low-passed u_* in Figure 22c.

The sediment profile timeseries spanning a 25 cm range to the bed during the same period are shown in Figure 23, with the bed at the bottom of the Figure, and the CASP head at the top. A two decade $\log_{10}$ scaling has been used to show the wide range of concentration and the rapid reduction with height above the bed for this measurement. Figure 24b represents the mass concentration timeseries estimated from the 1.3 MHz sonar range bin 1.5 cm above the bed. The low-passed shear velocity timeseries has been replotted in Figure 24a to show the very strong correlation between the periodic bursts of u_* and the sediment concentration. Figure 24c is the resulting X/Y component sediment flux timeseries at 36 Hz - net fluxes can be estimated from longer-term averages of this timeseries. The very high temporal resolution of the nonlinear mass-velocity flux product, $M \times (u,v,w)$, has been well resolved allowing the relationship between turbulent forcing parameters and mass flux to be explored.

This quality of measurement was obtained throughout the 15 day deployment in October 1994 at the Duck site, and promise to provide significant insight into the physics of sediment transport under a range of forcing conditions at sites spanning the shore, trough and bar system. The instrumentation performed without any electronic or mechanical difficulties

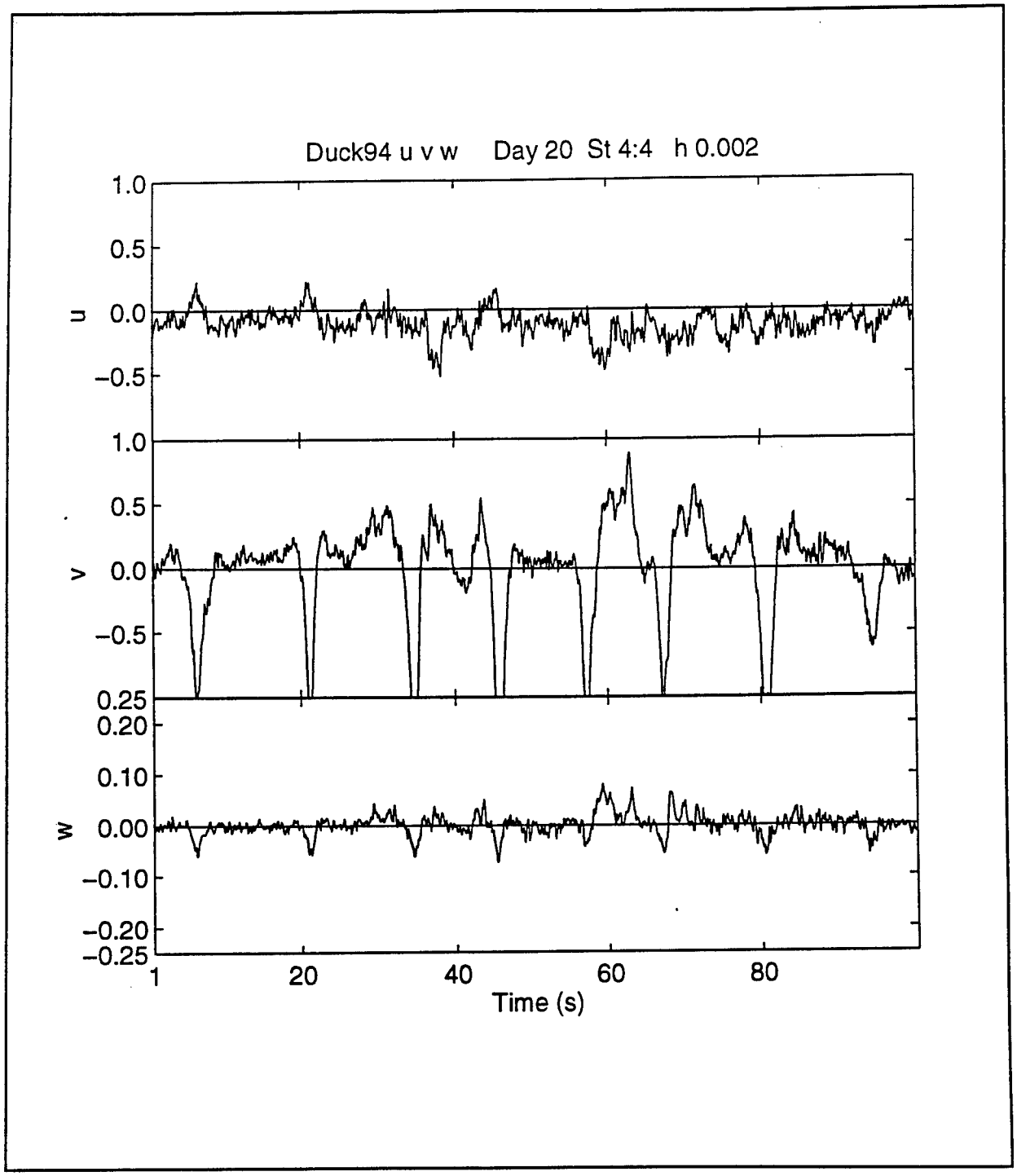

Figure 21 a - c. A 100 second timeseries of along-shore, u, cross-shore, v, and vertical, w, velocity components (ms^{-1}) measured by the CASP. These data were taken 187m offshore from the reference datum near the middle of the trough on 20 October 1994 under strong, narrow-band swell conditions.

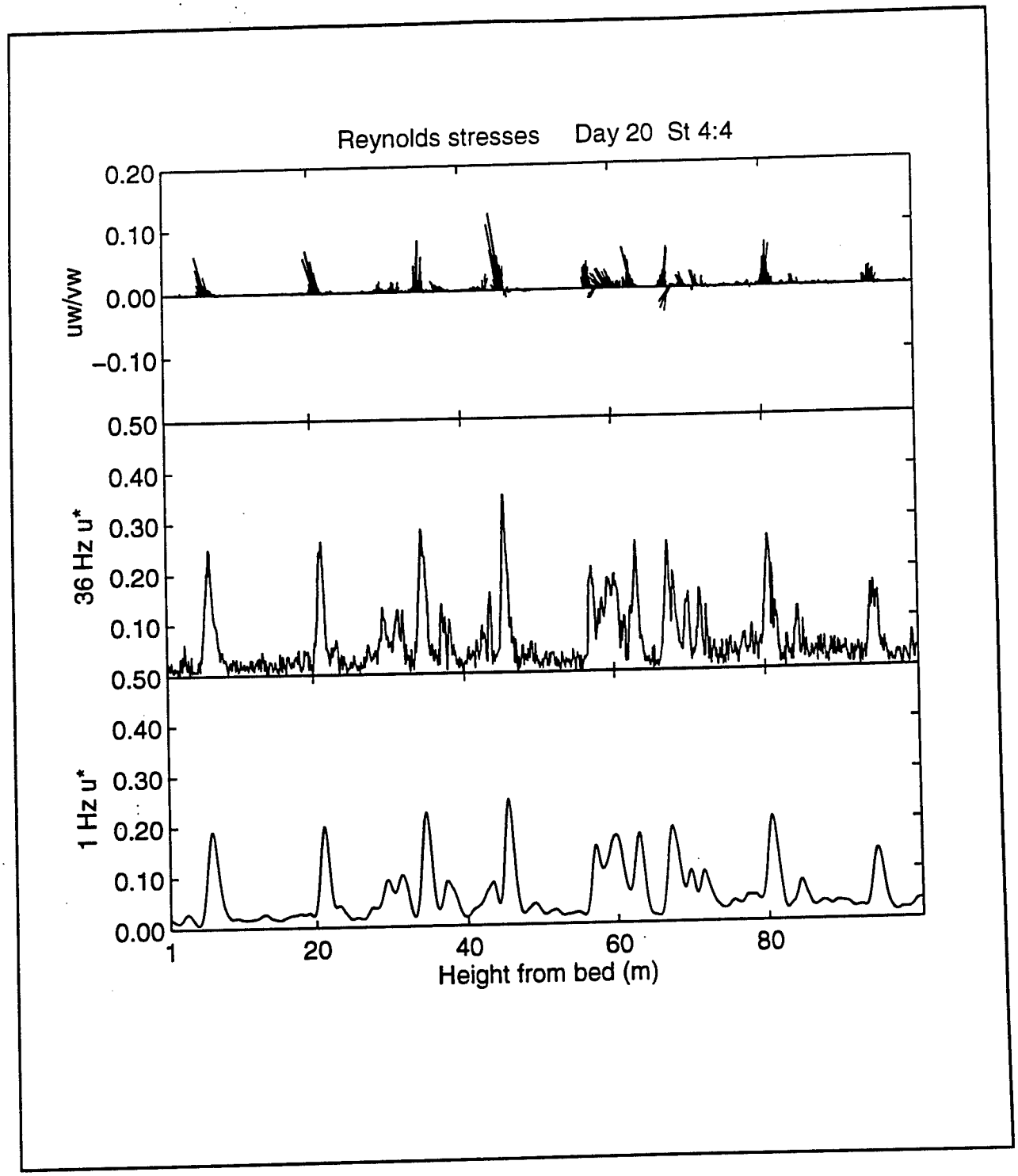

Figure 22 a - c. Reynolds stress vectors (m^2s^{-2}), shear velocity, u. (ms^{-1}) at 36 Hz, and u. low pass filtered at 1 Hz for the same period as Figure 21. Strong bursts of turbulent stress are associated with the highly nonlinear waves crossing the trough.

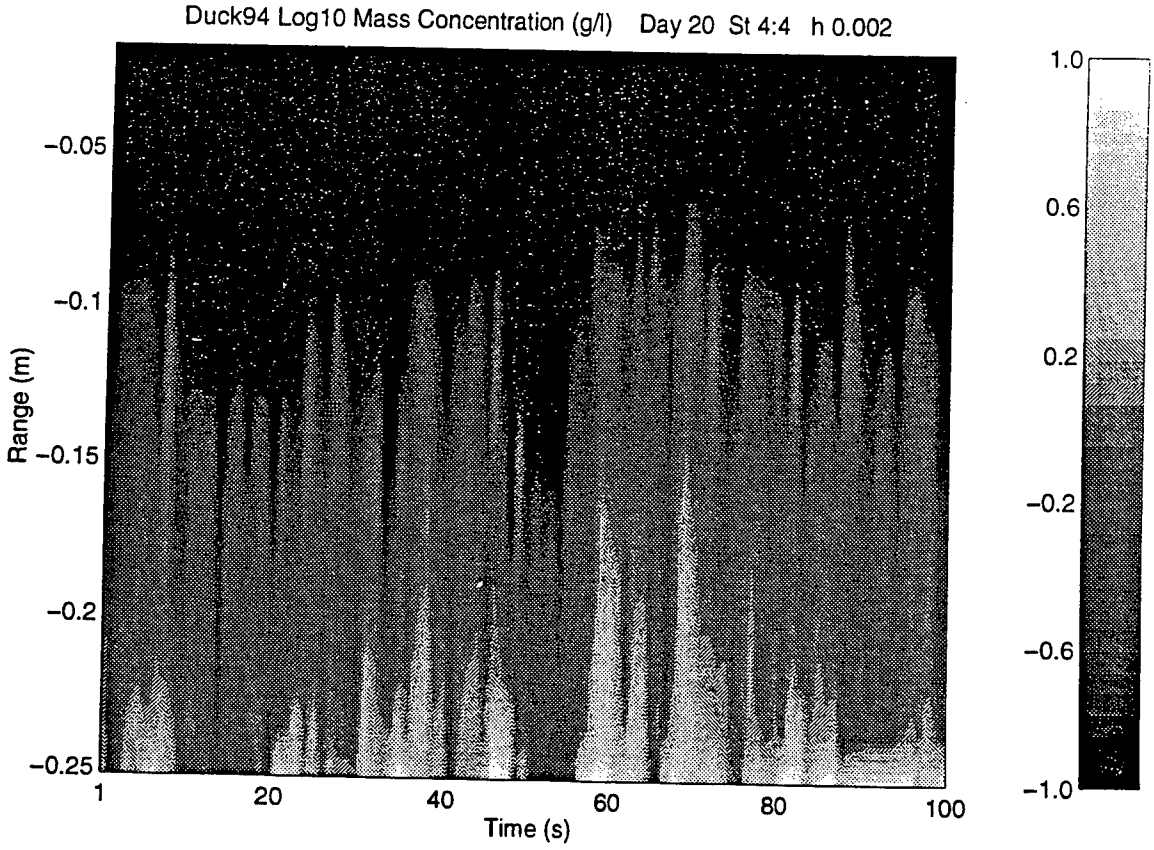

Figure 23. Log_{10} of mass concentration profiles for the same time as Figure 21. Sediment suspension events can be seen extending up from the bed with peak concentrations exceeding 10 g/l rapidly decreasing with height to less than .1 g/l

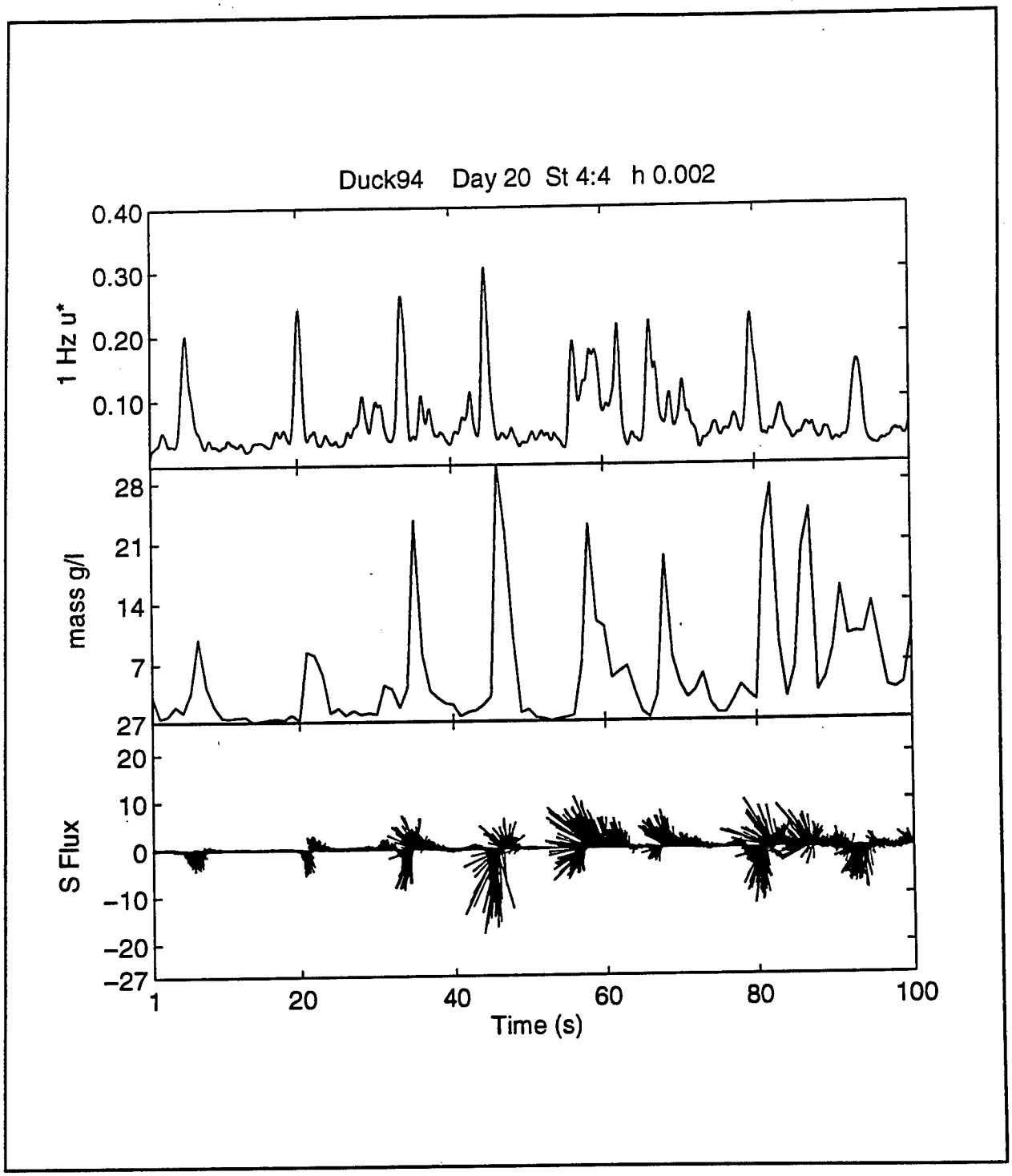

Figure 24a. 1 Hz low-pass filtered u. for the same period as Figure 21. 24b. Mass concentration 1.5cm above the sediment bed. 24c. The resulting X-Y mass flux vectors 1.5cm above the bed ($gl^{-1}ms^{-1}$), with high fluxes well correlated to the wave-forced stress events.

even under severe wave conditions. Both field and laboratory measurements suggest that the calibrations and processing algorithms developed for the CASP system are robust, and the combination of concurrent three component velocity vector and mass concentration measurements with a very small sample volume and high temporal have met the aims of this project.

References

Alonso, M. and E.J. Finn, 1967, Fundamental University Physics, Addison-Wesley.

Bedford, K.W., and O. Wai, D.M. Libicki and R. Van Evra, 1987, "Sediment Entrainment and Deposition Measurements in Long Island Sound", J. Hydraulic Engineering, ASCE, Vol 113, No. 10, 1325-1342.

Coelho, E.F., 1991, Acoustic sensing of ocean turbulence, M.S. Thesis, Naval Postgraduate School, pp.119.

Crawford, A.M., and A.E. Hay, 1991, "A comparison of two inversion methods for the determination of the concentration and sizes of suspended sand from multifrequency acoustic backscatter", EOS Trans., American Geophysical Union Fall Meeting, V72, n44, p230.

Hay, A. E., 1991, Sound Scattering from a particle-laden, turbulent jet", J. Acoustical Society of America, 90(4), 2055-2073.

Hay, A. and R.W. Burling, 1982, "On sound scattering and attenuation in suspensions, with marine applications", J. Acoustic Soc. of Amer. 72, 950-959.

Libicki, C. K.W. Bedford and J.F. Lynch, 1989, "The interpretation and evaluation of a 3-MHz acoustic backscatter device for measuring benthic boundary layer sediment dynamics", J. Acoustical Society of America, 85(4), 1501-1511.

Stanton, T.P., 1991, Subcentimeter resolution measurements of oceanic turbulence using an acoustic doppler backscatter probe, Paper 4AO6, ASA meeting, Houston JASA Vol. 90, p 2283.

Tamura, T. and D. M. Hanes, 1986, "Laboratory calibration of a 3MegaHertz acoustic concentration meter to measure suspended sand concentration", University of Miami, Rosentiel School of Marine and Atmospheric Science Tech. Rp 86-004

Young, R. A., J.T. Merrill, T.L. Clarke, and J.R. Proni, 1982, "Acoustic profiling of suspended sediments in the marine bottom boundary layer", Geophysical Research Letters, 9, 175-178.

APPENDIX A
Notation and Symbols

a	Sediment particle diameter	m
c	Speed of sound in water	ms^{-1}
C	Digitized acoustic receiver output	counts
Calmass	Sediment mass calibration coefficient	$Kg\ m^{-3}\ v^{-2}$
db	Decibals	no units
f	Frequency	Hz
F	Transmit frequency	Hz
K	Molecular diffusivity	$m2s^{-1}$
k	Acoustic wavelength	m^{-1}
l	Path distance	m
M	Mass concentration	$Kg\ m^{-3}$
r	Range	m
S	System sensitivity	v
t	Time	s
T	Water temperature	°C
U_j	j'th Velocity component	ms^{-1}
u'_j	j'th fluctuating velocity component	ms^{-1}
V	Receiver voltage amplitude	v
v_{BS}	Bistatic velocity component	ms^{-1}
W_s	Sediment vertical velocity	ms^{-1}
x_j	j'th distance coordinate	m
α_S	Sediment/water attenuation coefficient	m^{-1}
α_W	Water attenuation coefficient	m^{-1}
β	Angle from the transducer main lobe axis	°
ρ_S	Sediment density	$Kg\ m^{-3}$

APPENDIX B
CASP Software User's Manual

Introduction

This document provides information on how to use the CASPHOST/CASPDSP PC/DSP software. The CASPHOST program runs on a PC and controls and monitors a digital signal processor (DSP) card installed in the PC. The DSP selects specific channels of data in the input serial data stream, does filtering and other processing, then passes the data to the PC via the EISA bus in the PC. The PC then displays selected channels in a real-time graphical display and optionally writes the data to disk .

Set up of the CASPHOST program involves user editing of a parameter file which is read at program start time, and prompted user input from the keyboard. The remainder of this document will describe how to set up and run this program.

Running The Program

Start the program by executing:

casphost parmfile.prm

where parmfile.prm is the name of a parameter file. If no parameter file is entered on the command line, you will be prompted for a name by the program.

When the program is run, the information read from the parameter file is displayed. The user should confirm that the displayed information is correct before continuing. The first prompt allows the user to select real-time mode, data storage mode, or quit. Real time mode will plot data to the display only, data storage mode will plot data to the display and also write to disk.

If data storage is selected, the program will attempt to open a data file in the requested directory. Data files are numbered consecutively. The first file will be named cspts.0. The next available file number is stored in a file named caspdir.

A prompt for file length is displayed next. Enter the number of minutes to run the program. The program will record data in one file for this length of time, then quit. Alternatively, enter 0, then the program will run forever (until interrupted by the user) creating a new file every two hours.

The program will then display a list of items that can be selected for plotting. Up to 6

items may be plotted at one time. The program will prompt for the number of items to be plotted. Select a number between 0 and 6. If 0 is selected no data is plotted. This is sometimes useful in debugging when you wish to print information to the screen. If 1 or more items are selected, the program will prompt for a list of items to plot. Select the numbers associated with the parameters you wish to plot and enter them as a blank separated list followed by a carriage return, or enter each one separately followed by a carriage return. If any of the items you selected are not available because they were not turned on in the parameter file, you will be notified that some of your entries are invalid, and you should select other items.

The next prompt selects the time scale for the plots. Data is plotted oscilliscope fashion for the selected time, then the plots are redrawn. 20 seconds is a typical value.

The computer will now display plot frames for the plot items selected, and a prompt to press any key when you want to start your run.

The computer will then start to display the selected data. After the time scale has elapsed, the data will be erased, and new plots begun. A flashing smiley face is displayed in the upper right corner of the screen as long as data is coming into the computer from the instrument.

The keyboard is live, and pressing any key will display a menu of options. Data will continue to be written to disk if data recording has been selected.

Menus

The menu system includes the following options and submenus:

1) exit menus, restart graph
   (returns to the data plotting screen)
2) change data collection
   1) goto previous menu
   2) start/stop data collection to disk
3) change plotting parameters
   1) goto previous menu
   2) change the number of seconds on the x-axis
   3) change parameter(variable, min, span, ...)
      (displays all variables currently being plotted and allows the user to change any plot including selecting a new data type to plot or changing the y axis minimum and span)
   4) delete a graph
   5) add a graph
   6) display status of all graphs
      (ie displays what data types are currently being plotted and the y-axis plot

limits)
7) stop all graphing
4) display processing flags
(displays the information read from the parameter file when the program was started)
5) exit CASPHOST program

Data Types

The following data types are available for plotting:

- bistatic frequencies (6 channels)
- bistatic power (6 channels)
- bistatic bandwidth (6 channels)
- monostatic power profiles (4 beams)
- water pressure
- tilt a
- tilt b
- head temperature

Single value data types such as the bistatic quantities, u,v,w, tilts etc. are displayed as line plots with the y axis representing the level of the data being plotted, and the x axis representing time. Profile quantites are displayed as color shaded plots with the y axis representing distance along beam, the x axis representing time, and the color level representing the level of the data.

Setup Files

The CASPHOST program requires several setup files which normally do not require modification, and one parameter file which may require occasional changes.

Parameter File

This is an ASCII file that can be edited with any ASCII text editor. All the parameters in this file are described in some detail at the end of this document. The names of all the other setup files are listed in this file along with locations of output file directories, and various data collection enable/disable flags. If you want to change the directory where data is logged, edit this file and change the outdir parameter.

Despike Setup File

This file contains information for the DSP coded single point despike algorithim. An optimized version of this file is provided, and no further modification is required

Control File

This file contains information on the location of each data channel in the input data stream. This file is only changed if the instrument data sequencing EPROM is changed. A current version of this file is provided, and no further modification is required.

Default Plot Labels and Limits File

Contains the plot labels and the default y-axis limts.

PARAMETER FILE

This file is read at the beginning of the program to tell the software what data types to process, where to write data to disk, and where to look for other setup files. This file is ASCII text, and can be edited by any editor capable of reading and writing an ASCII text file. When editing the file make sure that long lines are not 'wrapped' to the following line. It is a good practice to keep lines less than 80 characters to avoid this problem.

Lines in the file can be blank, contain a comment indicated by a #, or contain a parameter name and value. Lines containing numeric parameters can have a comment on the same line beginning with a #. Lines containing string parameters cannot have comments on the same line.

For example, valid lines in a parameter file might look like:

```
# default casp parameter file
#
#    don't put comment on lines containing string arguments
#
# demean and deglitch file
#
confile c:\spool\casp1.con
dsid 0                          # data set id
```

The following parameters are defined for CASPHOST

pgm - the path and file name of an executable program that will be downloaded and run on the DSP.

confile - File name of the ASCII .con file containing offset and interval data for demultiplexing channels from the raw data. There will be a different confile for any new sequencer EPROM used in the instrument.

outdir - directory path name for local disk storage of program output data.

loutfile = filename prefix for output data files

The following parameters are all flags. Set to 1 to turn on the associated data for processing, set to 0 to turn off. NOTE: if a particular flag is not turned on, the associated data will not be written to disk by CASPHOST and it will not be available for plotting.

depth_on - depth channel

tilt1_on - tilt 1 channel

tilt2_on - tilt 2 channel

headtemp_on - heat temperature channel

bistat_on - turns on all processing of power, frequency and bandwidth for all 6 bistatic channels. This is required to calculate velocity components.

monostat1_on - turns on processing for monostatic beam 1

monostat2_on - same for beam 2.

monostat3_on - same for beam 3.

monostat4_on - same for beam 4.

mono_power - turns on backscatter intensity data output for the enabled beams. This is required to calculate sediment mass concentration profiles.

m_per_sec - number of monostatic intensity profiles output per second. Allowed values are 1, 2, or 4, and is typically 4.

APPENDIX C
CASPHOST Data File Format

Data files written by the CASPHOST program have a self documenting format that allows the record length to vary depending on the data types that are selected for processing in the CASPHOST parameter file. Data are written in approximately 1 second (exactly 36 sample) blocks.

Each block contains a header record and a data record. The header record includes the number of data types in that block, the data type id numbers, and the number of samples for that data type. The data record is divided into two sections. The first section contains 36 samples of each of the single value data types (eg. u, v, w, bistatic frequencies etc), and the second section contains the multiple bin data types (eg. monostatic power profiles and monostatic mass estimates). It is important to note that the data types that are written to a file will not change during a given run since they are determined by the parameter file that is read at the beginning of a run.

All data are written as 2 byte integer words.

Header Record

The following table represents the contents of the Header Record as it appears on disk:

Contents	Number of Words
Number of Data Types (*n*)	1
Data Type ID numbers	*n*
Samples per Block	*n*

The following table lists the Data Type ID numbers and the Samples per Block for each data type:

Data Type	ID number	Samples per Block
water pressure	4	36
tilt a	11	36
tilt b	12	36
head temperature	13	36
bistatic frequency ch1	101	36
bistatic power ch1	102	36

bistatic bandwidth ch1	103	36
bistatic frequency ch2	104	36
bistatic power ch2	105	36
bistatic bandwidth ch2	106	36
bistatic frequency ch3	107	36
bistatic power ch3	108	36
bistatic bandwidth ch3	109	36
bistatic frequency ch4	110	36
bistatic power ch4	111	36
bistatic bandwidth ch4	112	36
bistatic frequency ch5	113	36
bistatic power ch5	114	36
bistatic bandwidth ch5	115	36
bistatic frequency ch6	116	36
bistatic power ch6	117	36
bistatic bandwidth ch6	118	36
monostatic powers	202	-n

where n is 1,2, or 4 depending on the value m_per_sec in the .prm file.

Data Record

As noted above, the data record consists of two parts. The first part includes all single value data types (identified in the table above as those data types with 36 samples per block), and the second part includes all multiple bin data types (identified in the table above as those types with negative samples per block). Let *s* represent the number of single value data types listed in the header, and let ***m*** represent the number of multiple bin types listed in the header.

Part 1 (single value data types)

The following table represents the contents of part 1 of the Data Record as it appears on disk:

Contents	Number of Words
Data Type 1	36
Data Type 2	36
.	
.	
.	
Date Type *s*	36
Ancillary Data	36

The Ancillary Data includes the following items:

Ancillary Data element 1	(year-1900) * 100 + month
Ancillary Data element 2	day * 100 + hour
Ancillary Data element 3	minute * 100 + second

The remaining 33 words of Ancillary Data are blank

Part 2 (multiple bin data types)

Multiple bin data types contain n profiles of 68 bins, where n is the value of m-per-sec in the .prm file. The following table represents the contents of part 2 of the Data Record as it appears on disk:

Contents	Number of Words
Data Type *s*+1	See Below
Data Type *s*+2	See Below
.	
.	
.	
Data Type *s*+*m*	See Below

The multiple bin data types have the number of profiles encoded in the header. Either 1,2 or 4 profiles are present in a record depending on the m_per_sec flag value.

Monostatic power is calculated at a 1 - 4 Hz rate (ie 1 - 4 profiles in a data block), and each of the profiles has 68 bins. Consequently each of these data types will have 816 words. The order of words in the block is as follows:

sample 1 beam 1 bin 1
sample 1 beam 1 bin 2
.
.
.
sample 1 beam 1 bin 68
sample 1 beam 2 bin 1
.
.
.
sample 1 beam 2 bin 68
.
.
.
sample 1 beam 4 bin 68
repeat for sample 2 through 4.

APPENDIX D
CASP Postprocessing Program

Postcasp Program Overview

The POSTCASP program provides post-processing for data files produced by the CASPHOST program. Bistatic data is bandwidth sorted, filtered, then used to calculate 3 component velocities at the 25 cm range sample point of the instrument. The resulting velocity data can be referenced to an instrument relative coordinate system, or rotated into a horizontal plane, using the instrument's internal tilt sensors. The coordinate system used to calculate the (u,v,w) velocity components is shown in figure 25.

Monostatic data is used to calculate sediment profiles. Sediment profiles are produced for both the 1.3 MHz beam, and one of the 5 MHz beams. Data can be written to disk as one binary file containing both velocity and sediment data, or two ASCII files with one containing velocity data, and one containing sediment profiles.

Usage

```
postcasp input_file output_file_prefix parameter_file
```

where:

`input_file` is the name of a file produced by the casphost program with the *tilt1_on*, *tilt2_on*, *bistat_on*, *monostat1_on*, *monostat2_on*, and *mono_power* flags all set.

`output_file_prefix` is the name of the output file(s) that will be produced by this run of the postcasp program. If the value of `output_file_prefix` is file, the output file(s) will be file.bin if binary output was selected, or file.vel and file.sed if ASCII output was selected.

`parameter_file` is the name of a file containing the setup parameters described in the **Parameter File** section below. Sample rate, filter width, attenuation factors and calibration factors are all set in the parameter file.

Binary Output File Format

If binary output mode is selected, one output file is produced for each input file. Each

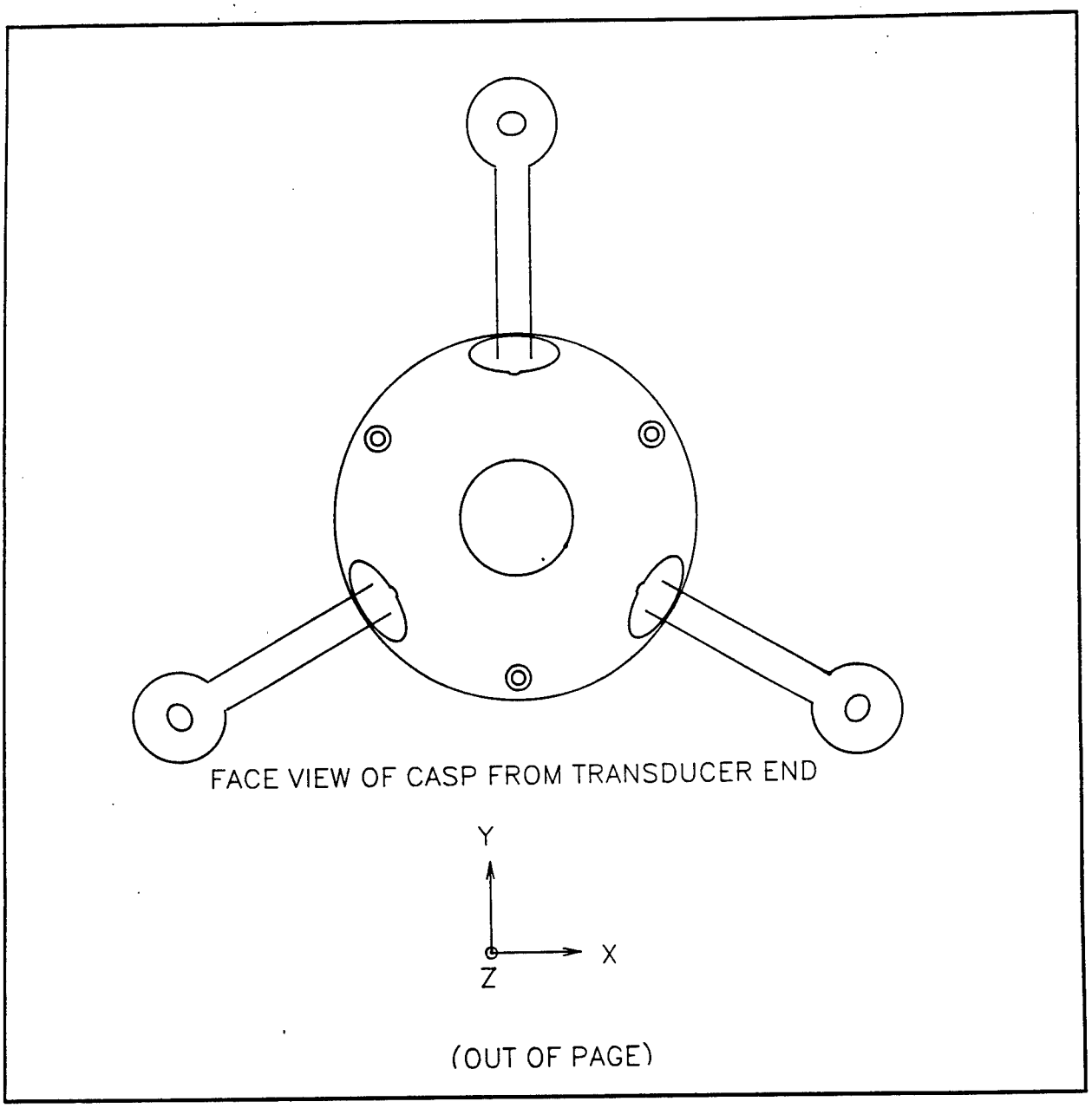

Figure 25. Schematic of the coordinate system used in the velocity vector calculation for the CASP. y (v) is alligned along the tranducer 1 arm, x (u) is 90° to the right, and z (w) is directed out of the page.

record in the file contains 1 second of data and includes a time tag, *nbist* samples of 3 component velocity (where *nbist* = 36/*sint*, and *sint* is set in the parameter file), *nsed* profiles each of sediment and backscatter intensity from beam 1, and *nsed* profiles of sediment and backscatter intensity from beam 2 (where *nsed* is the same as the *m_per_sec paramter* used when casphost was run). Each profile contains *nsedbins* bins of data. All data values are written as 2 byte 2's complement integers (ie short integers in C). Data has been scaled as necessary to fit within the range of a 2 byte integer.

- the first 3 values are *nbist, nsed, nsedbins* where
  - *nbist* is the number of bistatic estimates in the record
  - *nsed* is the number of sediment profiles in the record
- *nsedbins* is the number of bins in each sediment profile
- the next 6 values are year, month, day, hour, minute, and second
- next comes *nsed* profiles of backscatter data from beam 1, with each profile containing *nsedbins* values (counts squared). The first value in a profile is always the bin closest to the transducer.
- next comes *nsed* profiles of backscatter data from beam 2, with each profile containing *nsedbins* values (counts squared)
- next comes *nsed* profiles of sediment data from beam 1, with each profile containing *nsedbins* values (g/l)
- next comes *nsed* profiles of sediment data from beam 2, with each profile containing *nsedbins* values (g/l)
- the next *nbist* values are instrument coordinate u values, ($m\text{-}s^{-1}$ * 10,000)
- the next *nbist* values are instrument coordinate v values, ($m\text{-}s^{-1}$ * 10,000)
- the next *nbist* values are instrument coordinate w values, ($m\text{-}s^{-1}$ * 10,000)

ASCII Output File Format

If ASCII output mode is selected, two output files are produced for each input file. Velocity data from the bistatic mode are written to a file with a .vel extension, and sediment profile and backscatter data are written to a file with a .sed extension. This format has been designed with the MATLAB *load* command in mind. This command allows an ASCII flat file to be read directly into the MATLAB environment. A flat file is one which has the same number of blank separated values on each line. Some lines have been padded with zeros to accomplish this. In both files, each line is terminated by a linefeed character, and individual values are blank separated.

Velocity Data File

The first line in the file contains the number of velocity samples in a record (*nbist*), then each record after that consists of *nbist*+1 lines. Each record in the velocity file represents one

second of data, and contains a time tag, and *nbist* samples of velocity, where *nbist* = 36/*sint*, and *sint* is the sample interval for filtered data set by the user in the parameter file before the program is run. Velocities are $m\text{-}s^{-1}$.

The first line in the file will look like:

- *nbist* 0 0

where *nbist* will be a value like 18, 9, 6, 4, or 2. A single record would then look like:

- year*100+month day*100+hour minute*100+second
- u v w (sample 1)
- u v w (sample 2)
.
.
.
- u v w (sample *nbist*)

where each line above represents a linefeed terminated line in the data file

Sediment Data File

Each record in the sediment file represents one second of data and contains a time tag, *nsed* backscatter profiles for beam 1, *nsed* backscatter profiles for beam 2, *nsed* sediment profiles for beam 1, and *nsed* sediment profiles for beam 2. Each profile contains *nsedbins* bins where the first value in the profile is closest to the transducer. The value of *nsed* is determined by the *m_per_sec* parameter used in the CASPHOST parameter file, and *nsedbins* is normally 68. Each line in this file will be *nsedbins* long and will contain a profile. The time tag contains the *nsedbins* and *sed* values followed by time and padded with zeros.

- *nsedbins* nsed year month day hour minute second (followed by *nsedbins*-8 zeros)
- beam 1 backscatter profile 1, bin 1 to bin *nsedbins*
- beam 1 backscatter profile 2, bin 1 to bin *nsedbins*
- .
- .
- beam 1 backscatter profile nsed, bin 1 to bin *nsedbins*
- beam 2 backscatter profile 1, bin 1 to bin *nsedbins*
- beam 2 backscatter profile 2, bin 1 to bin *nsedbins*
- .
- .
- beam 2 backscatter profile, nsed bin 1 to bin *nsedbins*
- beam 1 sediment profile 1, bin 1 to bin *nsedbins*
- beam 1 sediment profile 2, bin 1 to bin *nsedbins*

- .
-.
- beam 1 sediment profile nsed, bin 1 to bin *nsedbins*
- beam 2 sediment profile 1, bin 1 to bin *nsedbins*
- beam 2 sediment profile 2, bin 1 to bin *nsedbins*
- .
-.
- beam 2 sediment profile nsed, bin 1 to bin *nsedbins*

with each line above represents a linefeed terminated line in the data file.

Parameter File

The parameter file is an ASCII file containing values of setup parameters for the program. The file is read once at the beginning of the program. Each line in the file contains a keyword followed by the value for that keyword. Blank lines can be included for clarity. Comment lines are preceded by a # character. Comments, preceded by a # can also be included on lines with numeric values, but not on lines with character values. When editing the parameter file, be very careful of editors that automatically line wrap. It is quite easy to have a comment line wrap around to the next line, so you have comments that are not preceded by a # character.

The currently defined parameters are:

tilt1_offset -- this is the 0th coefficient of a linear fit calibration of the tilt 1 sensor to convert instrument counts into degrees.

tilt2_offset -- same for the tilt 2 sensor.

tilt1_scale -- this is the 1st coefficient of a linear fit calibration of the tilt 2 sensor to convert instrument counts into degrees.

tilt2_scale -- same for the tilt 2 sensor.

calmass1 -- beam 1 sediment calibration factor ($g\text{-}l^{-1}\text{-}cts^{-2}$)

calmass2 -- same for beam 2

alpha1 -- beam 1 attenuation factor for the sediment type measured.

alpha2 -- beam 2 attenuation factor for the sediment type measured.

bw_lim -- this controls the data quality/filtering algorithm used in processing the velocity data by eliminating data which exceeds a bandwidth value of *bw_lim*. A typical value is 30, where bandwidth varies from 0, (good data), to 100 (bad data).

pwr_lim -- this controls the data quality/filtering algorithm used in processing the velocity data by eliminating data with acoustic backscatter power less than *pwr_lim*. A typical value is 3000.

fwidth -- this determines the width of the filter window applied to velocity data. This is the number of 36 Hz data points that are averaged together to generate data point for the output data file. Typically 8.

sint -- this determines the sample interval for the velocity data. This is the interval between data points in the output file, in terms of the 36 Hz input data. For example, if *sint* is 4, then the output data rate will be 36/4 = 9 Hz. Must evenly divide into 36, ie 4, 6, 9, 18. Typically fwidth/2, or the nearest equivalent.

rotate_flag -- this flag determines whether the velocity data will be rotated into a horizontal plane using the instrument tilt sensors, or left in a coordinate system aligned with the instrument. Set to 1 to rotate, or 0 for no rotation.

output_format -- this flag determines whether data is written to a binary format output file (0) or to ASCII format output files (1).

EXAMPLE

A typical file might look like the following:

```
# default parameter file for postcasp.

# tilt sensor calibration values

tilt1_offset  -0.00158622
tilt2_offset  0.00156306
tilt1_scale  0.07284468
tilt2_scale  0.033318198

# sediment calibration factors

calmass1  3.9e-8        # beam 1 sediment cal factor (g/l)/cts^2
calmass2  0.93e-8       # beam 2 sediment cal factor (g/l)/cts^2
alpha1 0.058            # beam 1, 1.2MHz  /m*(g/l)
alpha2 1.14             # beam 2, 5.2 MHz /m*(g/l)
```

```
# data quality and filtering parameters.
# bistatic data with bandwidth greater then
# bw_lim and power less than pwr_lim
# is rejected.  Data are filtered fwidth
# points at a time, (36 points per
# second), and velocity estimates are made
# every sint points.  Ie if
# fwidth=8, then the filter length is
# 8/36 or .222 seconds long.
# NOTE: sint must evenly divide into 36,
# ie 2, 4, 6, 9, 12, or 18
# If sint=4, the output velocity data will be 9 Hz.

bw_lim 30
pwr_lim 3000
fwidth 8
sint 4

# rotate_flag == 0, do not rotate.
# rotate_flage == 1, rotate.

rotate_flag 0

# output format == 0, then write to disk in binary mode.
# output format == 1, then write to disk in ascii mode.

output_format 1
```

APPENDIX E
Doppler Frequency Estimation

The bistatic velocity estimation requires a fast but accurate doppler spectral estimator. This estimator must rely on a small number of data points and be reliable even for weak signals submerged in strong noise. Several spectral estimators, including Peak FFT, Pulse Pair, Zero Cross, AR Model (order 4), MUSIC (order 4) and MUSIC (order 2), were analyzed and Monte-Carlo simulations performed to study their performances.

The use of spectral estimators to detect the presence of signals superimposed in white random noise demands a trade off between detectability and confidence of the detected values. The frequency estimator based on a finite number of data points represents an estimate of the true frequency that we would have if we had an infinite number of points. Therefore we need to characterize, in statistical terms, the behavior of these estimates. The Bias and Variance of the frequency estimates were used to compare the performance of several estimators.

Because determination of these statistics for a wide variety of algorithms is not analytically treatable, Monte Carlo simulations were used to obtain estimates of these statistics in terms of the Signal to Noise Ratio (SNR) of the input signal and of the record length used in the estimator. The results of this simulation have been used to determine the appropriate doppler frequency estimator, for the bistatic data stream.

The performance of an estimate can be assumed good when its bias is less than 1 Hz and the $\log_{10}$ of the standard deviation is less then 0. Using this criteria the following tables show the SNR at which the bias of the several estimators is equal to 1 Hz, and the log standard deviation equal to 0:

Because the CASP package bistatic doppler frequency estimation is based on 32 point records, and the algorithms run in real time using C compiled code in a DSP, the most suitable algorithms selected from these simulations are the PEAK FFT in the case of poor SNR, and the PULSE PAIR/MUSIC 2 algorithms for higher SNR. Considering discretization noise, the first choice for a spectral estimator for the CASP real time processing is the PULSE PAIR estimator, because of its computational performance, simplicity and high doppler frequency resolution.

TABLE 3. SNR at Bias = 1 Hz				
Estimator	20 Points	40 Points	60 Pointsr	80 Points
Peak FFT	-4	-5	-7	-8
Pulse Pair	-3	-8	-8	-8
Zero Cross	0	0	0	0
AR Model (order 4)	-2	-4	-5	-7
MUSIC (order 4)	2	-2	-5	-4
MUSIC (order 2)	-5	-6	-5	-8

TABLE 3. SNR at Variance = 1				
Estimator	20 Points	40 Points	60 Points	80 Points
Peak FFT	-3	-5	-7	-8
Pulse Pair	5	3	2	0
Zero Cross	5	4	3	2
AR Model (order 4)	8	0	-4	-5
MUSIC (order 4)	10	5	2	2
MUSIC (order 2)	5	3	2	0

REPORT DOCUMENTATION PAGE

Form Approved
OMB No. 0704-0188

1. AGENCY USE ONLY *(Leave blank)*	2. REPORT DATE	3. REPORT TYPE AND DATES COVERED
	September 1996	Final report

4. TITLE AND SUBTITLE
Coherent Acoustic Sediment Flux Probe

5. FUNDING NUMBERS

6. AUTHOR(S)
T. P. Stanton

7. PERFORMING ORGANIZATION NAME(S) AND ADDRESS(ES)
Naval Postgraduate School
Monterey, CA 93943

8. PERFORMING ORGANIZATION REPORT NUMBER

9. SPONSORING/MONITORING AGENCY NAME(S) AND ADDRESS(ES)
U.S. Army Corps of Engineers
Washington, DC 20314-1000

U.S. Army Engineer Waterways Experiment Station
3909 Halls Ferry Road, Vicksburg, MS 39180-6199

10. SPONSORING/MONITORING AGENCY REPORT NUMBER
Contract Report CERC-96-1

11. SUPPLEMENTARY NOTES

Available from National Technical Information Service, 5285 Port Royal Road, Springfield, VA 22161.

12a. DISTRIBUTION/AVAILABILITY STATEMENT

Approved for public release; distribution is unlimited.

12b. DISTRIBUTION CODE

13. ABSTRACT ***(Maximum 200 words)***

A high-resolution, three-component sediment flux probe has been developed to meet the objectives outlined by the National Academy of Science Panel on Coastal Engineering Measurements using very high-frequency coherent acoustic doppler techniques.

The Coherent Acoustic Sediment Flux Probe (CASP) system consists of an underwater housing equipped with three 5.2-MHz acoustic transceivers, a single 1.4-MHz transceiver, a pair of precision tilt sensors to correct package orientation tilts, and electronic processing and control modules which output a high-speed digital data stream to a shore-based processing computer. The instrument package is typically positioned looking downward at the bottom boundary layer to sample the velocity vector and sediment flux vector at a primary measurement volume 25 cm in front of the instrument head. In addition, profiles of sediment concentration are estimated every 1.68 cm along each of the four narrow acoustic beams.

Suspended sediment concentrations are inferred from profiles of acoustic backscatter acoustic intensity by measuring the range-gated power returns from the 1.3-MHz transceiver and each of the 5.2-MHz transceivers. The backscatter power

(Continued)

14. SUBJECT TERMS
Acoustic
Concentration profiles
Sediment transport
Suspension

15. NUMBER OF PAGES
74

16. PRICE CODE

17. SECURITY CLASSIFICATION OF REPORT	18. SECURITY CLASSIFICATION OF THIS PAGE	19. SECURITY CLASSIFICATION OF ABSTRACT	20. LIMITATION OF ABSTRACT
UNCLASSIFIED	UNCLASSIFIED		

13. ABSTRACT (Concluded).

levels are converted to sediment concentration profiles using an acoustic model which includes the effects of attenuation due to water and suspended mass, and radial spreading, to produce profiles from 6 cm in front of the instrument head to the sediment bed, up to a range of 1.2 m. Under restricted conditions, the ratio of backscatter measured by the 1- and 5-MHz transceivers can be used to identify changes in the mean sediment size.